Stony Brook University

Strange Stars in the MIT Bag Model

A Thesis Presented

by

Charlotte Mielke

to

The Graduate School

in Partial Fulfillment of the

Requirements

for the Degree of

Master of Arts

in

Physics

Stony Brook University

August 2011

Stony Brook University

The Graduate School

Charlotte Mielke

We, the thesis committee for the above candidate for the

Master of Arts degree, hereby recommend

acceptance of this thesis.

James Lattimer
Professor, Department of Physics and Astronomy,
Stony Brook University

Alan Calder
Assistant Professor, Department of Physics and Astronomy,
Stony Brook University

Maria Victoria Fernandez-Serra
Assistant Professor, Department of Physics and Astronomy,
Stony Brook University

This thesis is accepted by the Graduate School

Lawrence Martin
Dean of the Graduate School

Abstract of the Thesis

Strange Stars in the MIT Bag Model

by

Charlotte Mielke

Master of Arts

in

Physics

Stony Brook University

2011

We study strange stars under the assumption of the strange matter hypothesis, using an MIT bag model to describe strange matter. We find that a $1.97M_{\odot}$ star (as recently measured) is generally possible in the context of the bag model, although it places restrictions on the bag model's parameters. Furthermore, limits for the central pressure and energy density are obtained.

Contents

1 Introduction

The structure of a neutron star and its mass are determined by the underlying equation of state, but to date QCD has not been able to provide an equation that is valid for all densities and temperatures. With a typical radius of only 15 km and a mass of $1.5M_\odot$, neutron stars are among the densest objects in our universe, and it is not clear whether perturbation theories can be applied under these extreme conditions, where densities by far exceed the nuclear saturation density $n = 0.16$ fm^{-3}. Exotic types of matter such as strange matter, hyperons or kaon condensates have therefore been proposed to exist in the core of neutron stars, and the precise measurement of neutron star masses and radii is required to determine which of these conjectures is correct. In this sense, neutron stars are natural testing laboratories for matter under extreme pressures and densities.

A direct consequence of General Relativity is that there must be a maximum mass that no neutron star can exceed without collapsing into a black hole. The precise measurement of large neutron stars is therefore especially important, because it may rule out some equations of state that do not allow these masses and place severe restrictions on others, thereby helping us to gain more insight in the structure of matter under extreme pressures. Accurate measurements for neutron star masses are possible for pulsars in binary systems (mostly with another neutron star or a white dwarf) that are edge-on or have large eccentricities and large $\sin(\omega)$, where ω is the longitude of periastron. However, this only applies to very few pulsars in binaries. Less accurate measurements are possible for X-ray binaries. As a result of these difficulties, there are only very few accurately measured neutron star masses (for a list see [19]). Therefore, the measurement of a $(1.97M \pm 0.04)M_\odot$ pulsar, as reported in 2010 by Demorest et al. [8], is very exciting, as this by far exceeds the mass of the heaviest of the previously known neutron stars, $(1.667 \pm 0.021)M_\odot$ [29]), setting tight constraints on possible equations of state and thermodynamic quantities in neutron stars. The black widow pulsar might even have a mass of $2.4M_\odot$ [28], although this remains to be confirmed.

This thesis mainly focuses on the hypothetical existence of stable strange stars, i.e. stars that are made of $u-$, $d-$ and $s-$quarks. We use the MIT bag model to describe this kind of matter. The main goal of this thesis is to obtain restrictions on the properties of the bag model in the light of the recent mass measurements.

1.1 Structure of the thesis

In the first chapter, we introduce the Tolman-Oppenheimer-Volkov (TOV) equations, the equations for hydrostatic equilibrium in General Relativity, which govern a neutron star's structure. There are only very few analytic solutions to the TOV equations that fulfill basic requirements to physical stars, and we discuss one of them (the Buchdahl solution) in detail. We also dedicate some time to the incompressible fluid solution, which - although clearly unphysical - illustrates some features of relativistic stars. Since all other calculations in this thesis have to be numerical, we shortly describe the method that was used.

The second chapter is dedicated to the MIT bag model and the theoretical motivation for the existence of strange stars. After shortly touching on the classic MIT bag model as proposed by Chodos et al. [5], we discuss recent corrections for QCD, the strange quark mass and color superconductivity that lead to the equation of state that is used throughout this thesis. We then review the strange matter hypothesis by Witten [30] and analyze its implications on the parameters in the MIT bag model. Other models of strange quark matter are briefly mentioned as well.

In the third chapter, we want to explore how the maximum mass predicted by the MIT bag model depends on its parameters, especially in the light of the constraints that arise from the $1.97M_\odot$ star. We also analyze how the maximum mass scales with the bag model parameters.

The fourth chapter discusses thermodynamic properties that are relevant in neutron stars, such as pressure and energy density. It can be shown that the $1.97M_\odot$ star also places restrictions on these quantities.

Finally, there is a short summary of the results.

2 The Tolman-Oppenheimer-Volkov Equations

2.1 The TOV equations

Any stable star must be in hydrostatic equilibrium, i.e. there must be a balance between the thermal pressure and gravity, and the structure of a star is mainly determined by this requirement. The Newtonian equations for hydrostatic equilbrium

$$\frac{dp}{dr} = -\frac{m(r)\rho(r)}{r^2}, \tag{2.1}$$

$$\frac{dm}{dr} = 4\pi r^2 \rho(r), \tag{2.2}$$

where r is the radius, $m(r)$ is the enclosed gravitational mass, $p(r)$ is the pressure and $\rho(r)$ is the density at a given radius, become invalid for very compact objects such as neutron stars. Here, we must resort to General Relativity, and we replace the ρ by the energy density ε/c^2. Furthermore, in the following equations, we set $G = c = 1$. The equations for hydrostatic equilibrium in General Relativity are the Tolman-Oppenheimer-Volkov (TOV) equations, which are given by

$$\frac{dp}{dr} = -(\varepsilon + p)\frac{m + 4\pi r^3 p}{r(r - 2m)}, \tag{2.3}$$

$$\frac{dm}{dr} = 4\pi r^2 \varepsilon. \tag{2.4}$$

The equations can be derived from the Einstein equations assuming a general static, spherically symmetric metric

$$ds^2 = -e^{\nu(r)}dt^2 + e^{\lambda(r)}dr^2 + r^2(d\theta^2 + \sin^2\theta d\phi^2), \tag{2.5}$$

where

$$\lambda = -ln\left(1 - \frac{m(r)}{r}\right), \tag{2.6}$$

$$\nu'(r) = \frac{2p(r)}{\varepsilon(r) + p(r)}. \tag{2.7}$$

The prime denotes a derivative with respect to r. On the boundary of the star, a solution must match the Schwarzschild solution [23], i.e.

$$e^{\nu} = e^{-\lambda} = 1 - \frac{2M}{R}. \tag{2.8}$$

A solution to the TOV equation that could describe a physical star must fulfill certain criteria: For a star of radius R we must require that the pressure vanishes on the boundary $r = R$. For stars that are bound only by gravity, the energy density also has to vanish at the surface. Hypothetical self-bound stars could have a finite energy density at the surface, however [10]. Generally, pressure and energy density have to decrease monotonically as a function of r.

If we require causality (i.e. that the speed of sound be smaller than the speed of light), it is possible to show that no neutron star can have a mass that is larger than $3.2M_{\odot}$ [27]. Also, any specific equation of state $\varepsilon(r)$ has a maximum mass. Heavier stars are not stable and will collapse into black holes [19]. One goal of this thesis is to determine the maximum mass for the MIT bag model equation of state and analyze its dependence on the bag model's parameters in light of the recent measurement of a $1.97M_{\odot}$ neutron star [8].

2.2 Details of the numerical integrations

2.2.1 Integrating the TOV equations

Given an equation of state and a value for the central pressure p_c we can integrate the TOV equations numerically. For this, we use a fourth order Runge-Kutta method. Because the TOV equations are singular at the center of the star ($m = r = 0$), we use an incompressible fluid ($\varepsilon \equiv \varepsilon(0)$) as an approximation for small r, since there is an analytic solution in this case (see section 2.3.1). The integration stops when the pressure becomes negative, since we need $p > 0$ inside a star to prevent matter from falling towards the center due to gravitation.

This method can be improved by making the steps smaller as the integration approaches the surface of the star. Before each step of the integration, we calculate

$$p_t = p_n + p'_n \cdot \delta \tag{2.9}$$

where δ is the step size and p'_n is the slope at p_n as given by the TOV equations. If $p_t > 0$, then p_{n+1} will also be positive, so we have not yet reached the surface of the star, and we keep δ unchanged. If $p_t < 0$, then we have to adjust the step size by setting

$$\delta = -\frac{p_n}{2p'_n}. \tag{2.10}$$

The routine breaks when the step size is smaller than a given value. In this way, we can get

as close to the stellar surface as we want and thus obtain very accurate results. The problem is that it is impossible to know beforehand how many steps the routine has to execute to reach the desired level of accuracy. Of course, even without adjusting the step size, it is not clear from the beginning what the radius of the star will be, therefore, the number of steps can only be estimated before the integration, for example by using the equation of state for the incompressible fluid as an approximation (see section 2.3.1).

2.2.2 Modifications to the TOV equations

To avoid the problems explained above, the TOV equations can be modified [25] by introducing a new variable

$$dh = \frac{d\mu}{\mu} = \frac{dp}{\varepsilon + p} \tag{2.11}$$

and treating $m(h)$ and $r^2(h)$ as the dependent variables. The TOV equations are then given by

$$\frac{dr^2(h)}{dh} = -2r^2 \frac{r - 2m}{m + 4\pi p r^3}, \tag{2.12}$$

$$\frac{dm}{dh} = -4\pi\varepsilon r^3 \frac{r - 2m}{m + 4\pi p r^3}, \tag{2.13}$$

and they have to be integrated from the center $h(p_c) = h_c$ to the surface $h(p = 0) = 0$ of the star. At the center of the star ($h_c - h$ small), a power series expansion is possible [25]:

$$r^2(h) = \frac{3(h_c - h)}{2\pi(3p_c + \varepsilon_c)}, \tag{2.14}$$

$$m(h) = \frac{4}{\pi}\varepsilon_c r^3, \tag{2.15}$$

and it is used in the first step of the integration because both numerator and denominator tend to zero for r,$m \to 0$. Generally, 100 steps (or equivalently a step size of $h_c/100$) are sufficient. Because of these advantages, this is the method that will be used for the integrations in the following sections.

2.2.3 Finding the maximum mass

The maximum mass for a specific equation of state is a question of central importance. For both methods, we can calculate mass and radius for a given central pressure (or equivalently h_c). By iterating over different central pressures, we can obtain the mass versus radius relationship for any given equation of state. Of course, the above method only calculates discrete mass-radius pairs. Therefore, after calculating $30 - 100$ data pairs (depending on the

complexity of the equation of state), we apply a polynomial fit to the pairs in the environment of the largest mass. We then determine the maximum of said polynomial. Since the mass versus radius relationships for the equations of state discussed here are smooth, this simple method is sufficiently accurate. The calculation of more data pairs does not change the results appreciably.

2.2.4 Constants

To make the integration more accurate, we avoid the use of constants in the process. All results are therefore in units of km and can be converted to physical units via

$$1km = 1.50 \cdot 10^{-3} \sqrt{\frac{\mathrm{fm}^{-3}}{\mathrm{MeV}}}, \tag{2.16}$$

$$1M_{\odot} = 1.477 \text{ km}. \tag{2.17}$$

2.3 Analytic solutions to the TOV equations

There are only very few known analytic solutions to the TOV equations that fulfill the above requirements for gravitationally bound stars: the Tolman VII solution, the Buchdahl solution and the Narai 4 solution [20]. If we do not require the energy density to vanish at the surface, an infinite number of analytic solutions exists. In the following sections, we want to further examine the incompressible fluid solution ($\varepsilon(h) = const$) and the Buchdahl solution. Also, we will briefly touch on the Tolman VII solution.

2.3.1 The incompressible fluid

The easiest solution is the incompressible fluid with $\varepsilon(r) = a$ where a is a constant. Obviously, this solution does not satisfy all the above criteria because the energy density does not vanish on the surface. Solving the TOV equations leads to

$$m(r) = \frac{4\pi}{3}\varepsilon r^3, \tag{2.18}$$

$$p(r) = \frac{3\beta}{4\pi R^2}\frac{\sqrt{1-2\beta} - \sqrt{1-2\beta(r/R)^2}}{\sqrt{1-2\beta(r/R)^2} - 3\sqrt{1-2\beta}}, \tag{2.19}$$

where M and R denote the mass and radius of the star, respectively, and $\beta = M/R$. The central pressure is given by

$$p_c = \frac{3\beta}{4\pi R^2}\frac{\sqrt{1-2\beta} - 1}{1 - 3\sqrt{1-2\beta}}. \tag{2.20}$$

Another reason why this solution is unphysical is that the sound speed $c = \sqrt{\frac{\partial p}{\partial \varepsilon}}$ is infinite.

Nevertheless, it is interesting because it illustrates a general feature of General Relativity: The central pressure of the star becomes infinite if $\beta < 4/9$. It is possible to show that this limit is valid for any equation of state [12]. For more realistic models, we expect $\beta < 1/3$ [18], [11]. Note that $\beta < 1/2$ (i.e. the radius is larger than the Schwarzschild radius) is in any case required by General Relativity, otherwise the star would collapse into a black hole.

We use the modified TOV equations 2.13 for the integration. In this case

$$h(p) = \int_0^p \frac{dp'}{\varepsilon(p') + p'} = \ln(p + a) \tag{2.21}$$

$$\Rightarrow p(h) = e^h - a. \tag{2.22}$$

$\varepsilon(p)$ is independent of p and therefore $\varepsilon(h)$ is also independent of h. Figure 2.1 shows the calculated mass-radius relationship.

For comparison, we also integrate the Newtonian equations 2.2 in this case. The result for $m(r)$ remains unchanged, and we arrive at

$$\frac{dp}{dr} = -\frac{4}{3}\pi r \varepsilon^2 \tag{2.23}$$

$$\Rightarrow p(r) = \frac{2}{3}\pi R^2 \varepsilon^2 \left(1 - \frac{r^2}{R^2}\right) = p_c \left(1 - \frac{r^2}{R^2}\right), \tag{2.24}$$

where the central pressure of the star is given by

$$p_c = \frac{3\beta^2}{8\pi R^2}. \tag{2.25}$$

The solution (equation 2.24) is the first term in a power series expansion in β of equation 2.20, the next term being

$$\frac{3\beta^3}{4\pi R^2}\left(1 - \frac{r^2}{R^2}\right), \tag{2.26}$$

which means that the central pressure is always larger for General Relativity. Figure 2.2 shows the distance from the star's center versus pressure relation for both theories.

2.3.2 The Tolman VII solution

Another equation of state that has an analytic solution is

$$\varepsilon = \varepsilon_c \left(1 - \frac{r}{R^2}\right). \tag{2.27}$$

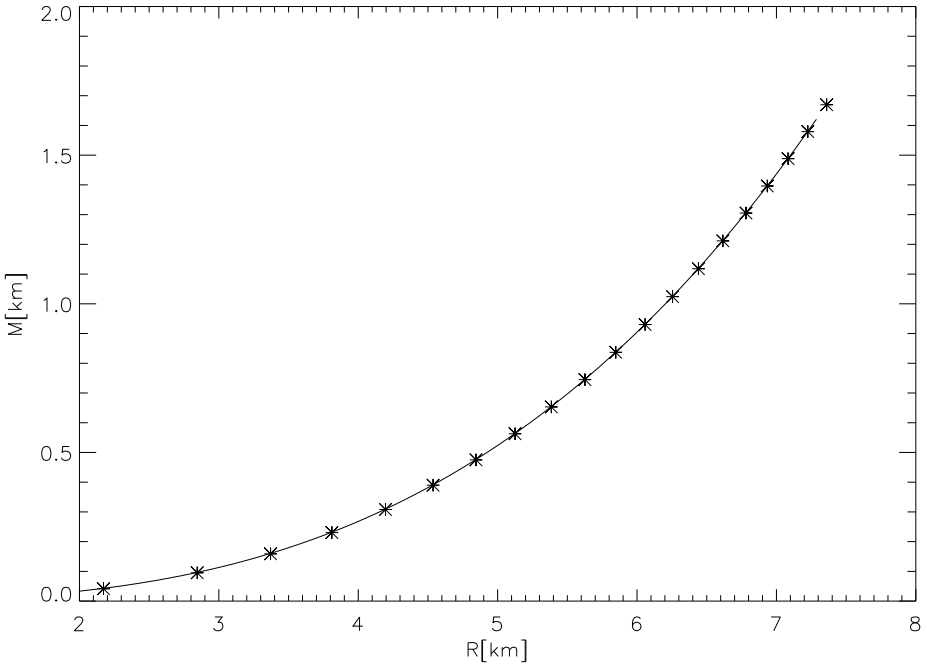

Figure 2.1: Mass versus radius relation for the incompressible fluid with $\varepsilon = 0.001$. The continuous line represents the analytic solution, the data points are the numerical integration.

It is known as the Tolman VII solution and requires $\beta < 0.3868$ for a finite central density and $\beta < 0.2698$ for causality [17]. The Tolman VII solution is of particular interest because it might set an upper limit for the central density for a given mass for any realistic equation of state [20]. Specifically, the central density is given by [20]

$$\varepsilon_c = 8.18 \, \frac{\text{GeV}}{\text{fm}^3} \cdot \left(\frac{M_\odot}{M} \right)^2 , \tag{2.28}$$

so $M_{\max} > 1.97 M_\odot$ requires $\varepsilon_c < 2.108$ GeV/fm^3.

2.3.3 The Buchdahl solution

The Buchdahl solution is another analytic solution to the TOV equations [17]. The equation of state is given by

$$\varepsilon = 12\sqrt{p_* p} - 5p. \tag{2.29}$$

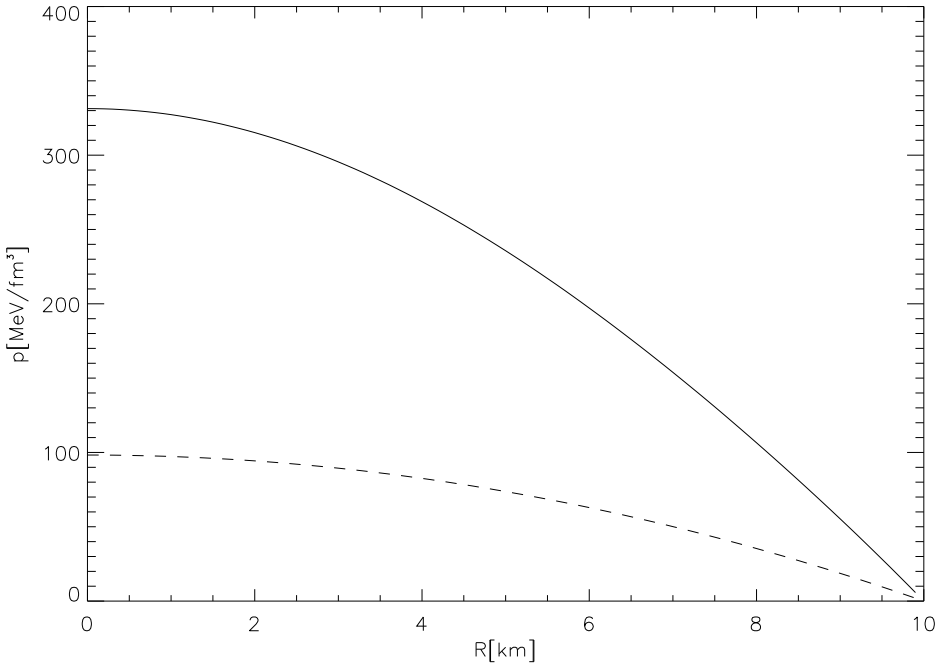

Figure 2.2: Distance from the star's center versus pressure relation for the incompressible fluid for Newtonian theory (dashed line) and General Relativity (solid line) with $\beta = 0.2$ and $R = 10km$.

Here, p_* is a constant. Obviously, we must require that

$$\sqrt{p_*} > \frac{5}{12}\sqrt{p}, \tag{2.30}$$

otherwise $\varepsilon < 0$. Figure 2.3a shows the equation of state for $p_* = 0.001$ km^{-2}. Another requirement is that the speed of sound

$$c_s^2 = \frac{1}{\partial\varepsilon/\partial p} = \left(6\sqrt{\frac{p_*}{p}} - 5\right)^{-1} \tag{2.31}$$

be smaller than the speed of light. This implies $p_* > p$. Furthermore, we need $c_s^2 > 0$, so

$$\sqrt{p_*} > \frac{5}{6}\sqrt{p} \tag{2.32}$$

There is an implicit relation between M and R which is given by

$$R = (1-\beta)\sqrt{\frac{\pi}{288 p_*(1-2\beta)}}. \tag{2.33}$$

.

A series expansion in β gives

$$R = \frac{1}{\sqrt{p}} \cdot \left(\sqrt{\frac{\pi}{288}} + \sqrt{\frac{\pi}{1152}} \beta^2 + O(\beta^3) \right), \tag{2.34}$$

which means that an increase in mass will result in only a small increase in radius.

Equation 2.33 can be written as a quadratic equation in M:

$$M^2 + M \left(-2R + 2 * \frac{288 p_*}{\pi} R^3 \right) + R^2 - \frac{288 p_*}{\pi} R^4 = 0, \tag{2.35}$$

which has a (real) solution if and only if

$$R > \sqrt{\frac{\pi}{288 p_*}}. \tag{2.36}$$

Consequently, there is a minimum radius for the Buchdahl solution that depends on p_*.

The central pressure and energy density are given by [17]:

$$p_c = 36 p_* \beta^2, \tag{2.37}$$

$$\varepsilon_c = 72 p_* \beta (1 - 5\beta/2). \tag{2.38}$$

The requirement $p_* > p_c$ that results from causality therefore implies that

$$\beta < \frac{1}{6}. \tag{2.39}$$

However, $\varepsilon > 0$ already requires $\beta < 2/5$. Because of these limits, the Buchdahl solution not only has a minimum radius, but there is also a maximum radius for any p_*: Since $(1-\beta)/\sqrt{1-2\beta}$ increases monotonically for $0 < \beta < 2/5$ (see figure 2.4), the requirement of $\beta < 2/5$ means that $R \lesssim \frac{0.14}{\sqrt{p_*}}$, and for $\beta < 1/6$, we even have $R \lesssim \frac{0.10}{\sqrt{p_*}}$. So the Buchdahl solution is only applicable to a very narrow range of radii. A direct consequence is that

$$M_{\max} < \frac{1}{6} R < \frac{0.02}{\sqrt{p_*}}. \tag{2.40}$$

For the numerical integration, we need

$$h(p) = \int_0^p \frac{dp}{12\sqrt{p_* p} - 4p} = -\frac{1}{2} \ln\left(1 - \frac{\sqrt{p}}{3\sqrt{p_*}}\right) \tag{2.41}$$

$$\Rightarrow p(h) = 9p_*(1 - e^{-2h}). \tag{2.42}$$

$\varepsilon(h)$ can be obtained using equation 2.29. Figure 2.3b shows the results of the integration for $h = 0.6$ and figure 2.5 shows the mass versus radius relationship.

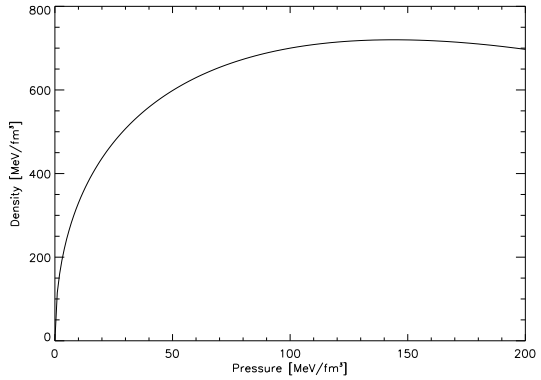

(a) Equation of state for the Buchdahl solution for $p_* = 0.001$ km^{-2} = 755.86 $\frac{\text{MeV}}{\text{fm}^3}$

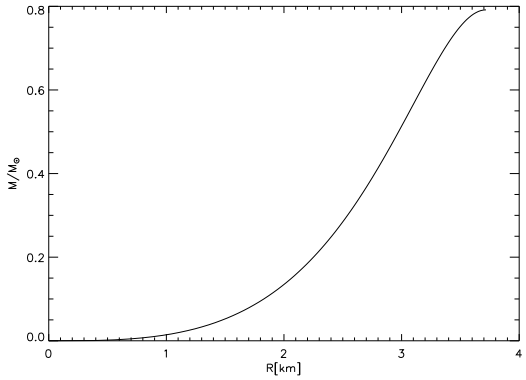

(b) Enclosed mass versus distance from the center for $p_* = 0.001$ km^{-2}, resulting in a star with $M = 0.79 M_\odot$ and $R = 3.72$ km

Figure 2.3: The Buchdahl solution.

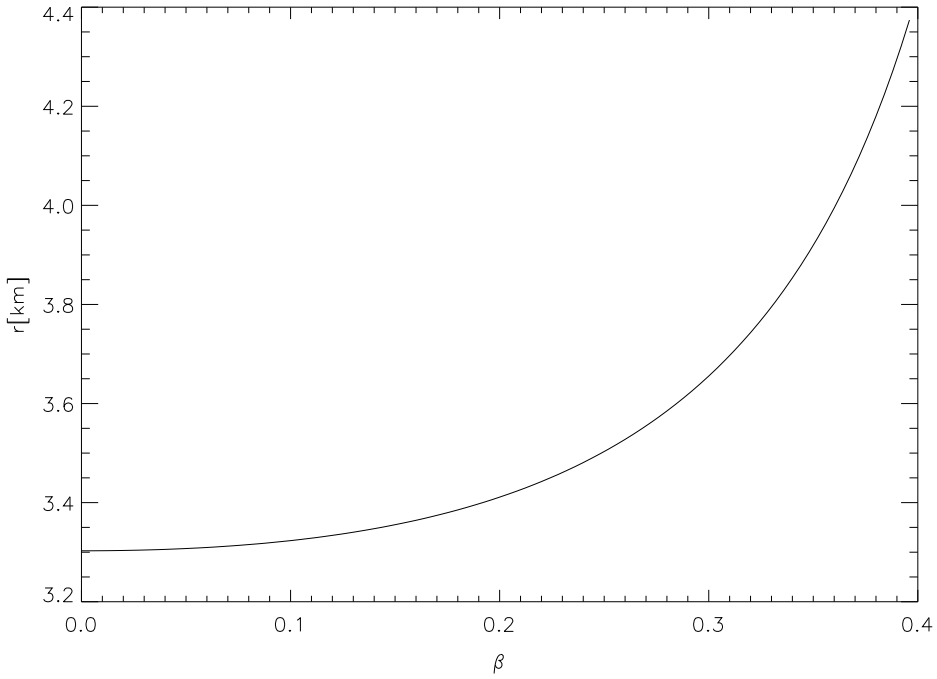

Figure 2.4: Equation 2.33 for $p_* = 0.001$ km^{-2}

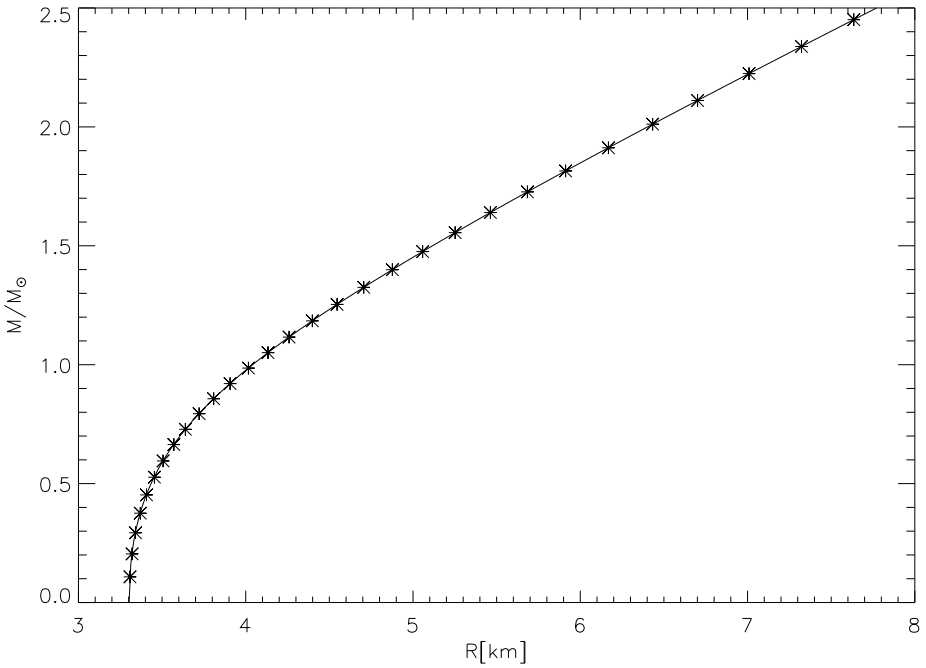

Figure 2.5: Mass versus radius relation for the Buchdahl solution with $p_* = 0.001$ km^{-2}. The continuous line represents the analytic solution, the data points are the numerical integration. Note the minimum radius $R_{\min} = 3.30$ km from equation 2.36, and the maximum radius (using $\beta < 2/5$) is $R_{\max} = 4.23$ km, resulting in a maximum mass of about $1.05 M_\odot$.

3 The MIT bag model and quark stars

The structure of any compact star crucially depends on the equation of state. Therefore, this chapter gives a brief introduction to the MIT bag model which is mainly used throughout the thesis. We then shortly discuss the strange matter hypothesis and its implications in the bag model. Finally, there is a short discussion of other hadron models.

3.1 The classic MIT bag model

The bag model provides a phenomenological description of hadrons. Essentially, the bag model assumes that the quarks are confined to a sphere of a certain radius (the bag), inside of which they are treated as massless free particles. The idea stems from the fact that single quarks have never been observed. It is necessary to intodruce a bag constant, which can be interpreted as the vacuum pressure on the bag surface that stabilizes the system. Radius and mass of the nucleus can then be expressed as

$$R = \left(\frac{2.04N}{4\pi B}\right)^{1/4}, \tag{3.1}$$

$$M = \frac{4}{3}(4\pi B)^{1/4}(2.04N)^{3/4}, \tag{3.2}$$

where N is the number of quarks in the bag and B is the above-mentioned bag constant. Experimentally known masses can then be used to fit B. Although the results are generally in agreement with experimental data [15], there is a wide range of possible values for B [9], [3].

To solve the TOV equations, it is necessary to derive the equation of state for the bag model [31]. The baryon density in a neutron star is very high, therefore we need to consider a relativistic degenerate quark gas. The number of states within the momentum interval $[p,p+dp]$ in a volume V is given by

$$\frac{g_q V}{(2\pi)^3} 4\pi p^2 dp. \tag{3.3}$$

Here, g_q is the degeneracy number of the quark gas. It is given by

$$g_q = 3 \cdot 2 \cdot \begin{cases} 2 & \text{for nonstrange matter} \\ 3 & \text{for strange matter} \end{cases} \tag{3.4}$$

Equation 3.3 can be integrated and divided by V to give the quark number density

$$n_q = \frac{g_q}{6\pi^2}\mu_q^3. \tag{3.5}$$

Likewise, we can obtain the energy density, where the bag constant enters to account for the vacuum pressure on the bag:

$$\varepsilon_q = \frac{g_q}{24\pi^2}\mu_q^4 + B \tag{3.6}$$

and the pressure

$$p_q = \frac{g_q}{24\pi^2}\mu_q^4 - B. \tag{3.7}$$

Note that there is a transition to quark-gluon plasma when $p_q = 0$. At that point, the inward bag pressure is no longer able to balance the outward pressure from the degenerate quark gas, resulting in deconfinement of the quark matter. Here, the transition will occur for a baryon density of

$$n_B = \frac{1}{3}n_q = \frac{4}{3}\left(\frac{g_q}{24\pi^2}\right)^{1/4} B^{3/4}. \tag{3.8}$$

3.2 The bag model equation of state

A somewhat more sophisticated quark matter equation of state can be obtained by a power series expansion in the quark chemical potential μ [2]:

$$p = \frac{3}{4\pi^2}a_4\mu^4 - \frac{3}{4\pi^2}a_2\mu^2 - B_{\text{eff}} \tag{3.9}$$

The quartic coefficient is given by $a_4 = 1 - c$ where c represents QCD corrections. For free noninteracting quarks we expect $c = 0$ or $a_4 = 1$. Otherwise

$$a_4 = 1 - \frac{2\alpha_c}{\pi} \tag{3.10}$$

where α_c is the QCD coupling [9]. Perturbative calculations find $a_4 \approx 0.63$, but it is not clear whether this is accurate in the context of compact stars [2].

The effective bag constant B_{eff} accounts for the free energy contribution that is independent of μ. In the following chapters, we will consider B_{eff} as a mere parameter. In the context of hybrid stars, it may be more reasonable to fix the density ρ_t at which the transition from nuclear matter to quark matter occurs [2] and take the effective bag constant as dependent on a_4, a_2 and ρ_t.

The quadratic coefficient a_2 arises because of the strange quark mass and color superconductivity. Specifically, it is given by

$$a_2 = m_s^2 - 4\Delta^2 \tag{3.11}$$

where m_s is the strange quark mass and Δ is the pairing gap that arises for color flavor locked (CFL) matter. The meaning of a_2 can be explained as follows [2]: The free energy of unpaired quark matter is given by

$$\Omega_{\rm unp} = \frac{3}{\pi^2} \sum_{i=u,d,s} \int_0^{\sqrt{\mu_i^2 - m_i^2}} dp p^2 (\sqrt{p + m_i^2} - \mu_i) + B_{\rm eff}. \tag{3.12}$$

μ_u, μ_d and μ_s denote the $u-$, $d-$ and $s-$quark chemical potentials, respectively. m_i denote the quark masses, but in the following the $u-$ and $d-$quarks are considered massless. Effectively, there is only one independent chemical potential: Two are fixed by the condition of chemical equilibrium which is maintained by the weak interaction processes

$$d \leftrightarrow u + e + \bar{\nu}_e, \tag{3.13}$$

$$s \leftrightarrow u + e + \bar{\nu}_e, \tag{3.14}$$

$$s + u \leftrightarrow u + d, \tag{3.15}$$

specifically

$$\mu_d = \mu_s = \mu_u + \mu_e \equiv \mu, \tag{3.16}$$

where μ_e is the electron chemical potential.

Furthermore, bulk matter must be electrically neutral, which requires

$$\frac{2}{3} n_u - \frac{1}{3} n_d - \frac{1}{3} n_s - n_e = 0, \tag{3.17}$$

and this fixes another chemical potential. Using these conditions, we can obtain a series expansion in μ/m_s for the electron chemical potential m_s/μ, assuming that $m_s < \mu$:

$$\mu_e = \frac{m_s^2}{4\mu} - \frac{m_s^4}{48\mu^3} + O\left(\frac{m_s^6}{\mu^5}\right). \tag{3.18}$$

If we substitute this in the expression for the free energy of unpaired matter (equation 3.12), we obtain the free energy for neutral, unpaired bulk matter:

$$\Omega_{\rm unp}^{\rm neut} = -\frac{3a_4}{4\pi^2}\mu^4 + \frac{3\mu^2 m_s^2}{4\pi}. \tag{3.19}$$

Terms of higher order in m_s/μ have been omitted. It can be shown that this series converges rapidly, even if m_s is not much smaller than μ, but this does not work for charged unpaired matter [2].

In CFL matter, the number densities of the quarks are required to be equal, and this lowers the free energy to [2]

$$\Omega_{\text{CFL}} = \Omega_{\text{unp}} - \frac{3}{4\pi^2}\Delta^2\mu^2. \tag{3.20}$$

Combining these two equations yields $a_2 = m_s^2 - 4\Delta^2$.

3.3 Solving the TOV equations for the MIT bag model

First, consider $a_2 = 0$ (thus neglecting the strange quark mass and superconductivity). In this case,

$$\varepsilon = \frac{\partial p}{\partial \mu}\mu - p = \frac{9a_4}{4\pi^2} + B_{\text{eff}}, \tag{3.21}$$

so this equation of state is given by

$$\varepsilon(p) = 3p + 4B_{\text{eff}}, \tag{3.22}$$

independent of a_4. This gives

$$h(p) = \frac{1}{4}\ln\left(4p + B_{\text{eff}}\right) \tag{3.23}$$

$$\Rightarrow p(h) = \frac{1}{4}(e^{4h} - B_{\text{eff}}). \tag{3.24}$$

The shape of the $M - R$ curve can be seen in figure 3.1.

For the case including a_2, the energy density is given by

$$\varepsilon = \frac{9a_4}{4\pi^2}\mu^4 - \frac{3a_2}{4\pi^2}\mu^2 + B_{\text{eff}} \tag{3.25}$$

and the number density is given by

$$n = \frac{3a_4}{\pi^2}\mu^3 - \frac{3a_2}{2\pi^2}\mu. \tag{3.26}$$

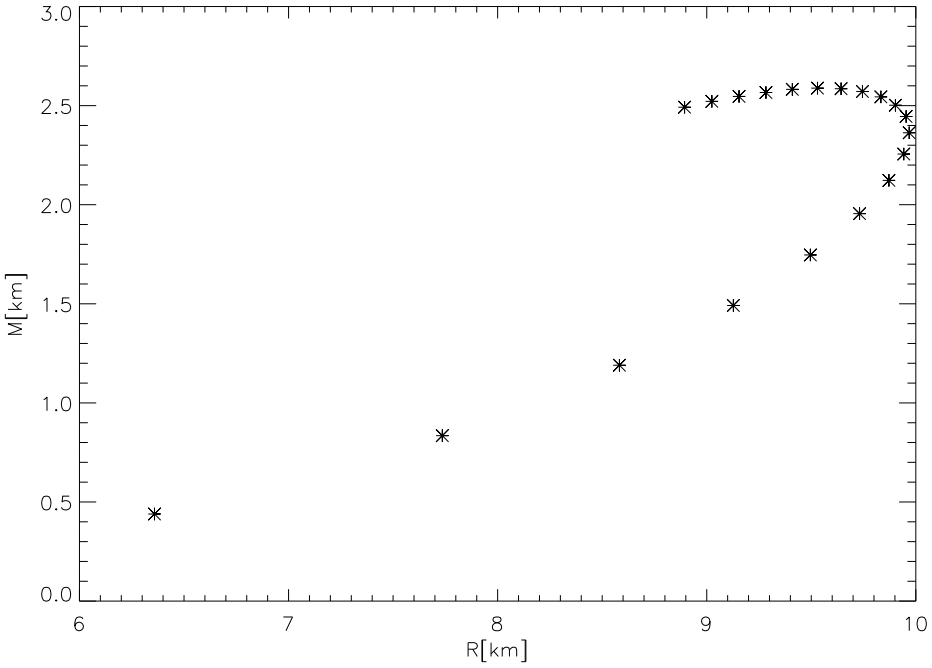

Figure 3.1: The $M - R$ relationship for the bagmodel for $B_{\text{eff}}^{1/4} = 155$ MeV, $a2 = 0$ MeV^2. Here, the value of a_4 does not influence the equation of state (see text). In this case, $M_{\max} \approx 2.55$ km $= 1.72 \mathrm{M}_{\odot}$.

The relations can be obtained via

$$n = \frac{\partial p}{\partial \mu}, \tag{3.27}$$

$$\varepsilon = n\mu - p. \tag{3.28}$$

Figure 3.2 shows the μ versus pressure and energy density relationships. Note that the pressure-energy density relation appears to be linear, even if a_2 is included (see figure 3.3). This is easily understood by expressing the energy density in terms of the pressure

$$\varepsilon = 3p + 4B_{eff} + \frac{a_2(3a_2 + \sqrt{9a_2^2 + 48a_4(B_{eff} + p)\pi^2})}{4a_4\pi^2} \tag{3.29}$$

$$= 3p + 4B_{eff} + \frac{\sqrt{3(B_{eff} + p)}a_2}{\sqrt{a_4}\pi} + O(a_2^2) \tag{3.30}$$

and one sees that the additional term is rather small and furthermore depends weakly on p.

If $a_2 = (0 \text{ MeV})^2$, the slope is 3 and the axis intersection is B_{eff}, independent of a_4.

To solve the TOV equations in the case, we first have to calculate the value μ_0 that corresponds to μ at $p = 0$ for each set of parameters a_4, a_2 and B_{eff}. This does not pose any problems because $p(\mu)$ is a quadratic equation in μ^2. From this we use equation 2.11 to obtain

$$\mu(h) = \mu_0 e^h. \tag{3.31}$$

Equations 3.9 and 3.25 are then used to determine $p(h)$ and $\varepsilon(h)$.

Figure 3.4 shows the relation between the enclosed mass and the distance from a star's center for different values of h_c. Each of these lines ends at the surface of the star. For these parameters, $h_c = 0.452$ leads to the maximum mass ($1.88 M_\odot$). This corresponds to a central pressure of 195.44 MeV/fm^3. Accordingly, $h_c = 0.6$ (equivalent to a central pressure of 387.24 MeV/fm^3) does not yield a stable configuration. Figure 3.5 shows the pressure and energy density versus distance from the star's center relation. Here, the the dotted and the dashed lines represent the maximum mass configuration for the given parameters. Again, the end of a line denotes the center of the star. Note that the energy density does not vanish at the surface of the star, but it can be calculated by substituting μ_0 in equation 3.25. Interestingly, the energy density function is very similar for (i) $B_{\text{eff}}^{1/4} = 145$ MeV and $h_c = 0.6$ and (ii) $B_{\text{eff}}^{1/4} = 165$ MeV and $h_c = 0.471$, although the maximum masses are very different: $1.82 M_\odot$ for (i) and $1.48 M_\odot$ for (ii).

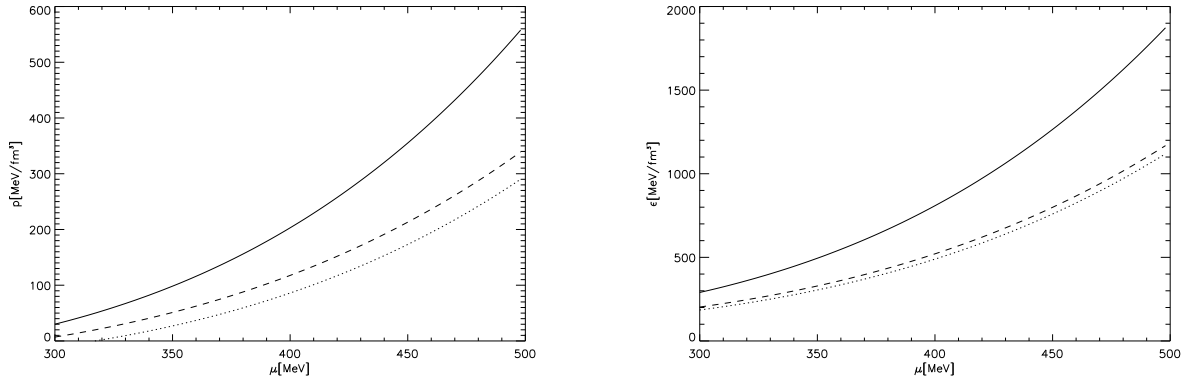

(a) $\mu - p$ relation **(b)** $\mu - \varepsilon$ relation

Figure 3.2: MIT bag model equation of state with $B_{\text{eff}} = (140 \text{ MeV})^2$ for $a_4 = 1.0$, $a_2 = 0.0$ MeV^2 (solid line), $a_4 = 0.6$, $a_2 = (100 \text{ MeV})^2$ (dotted line) and $a_4 = 0.6$, $a_2 = -(100 \text{ MeV})^2$ (dashed line).

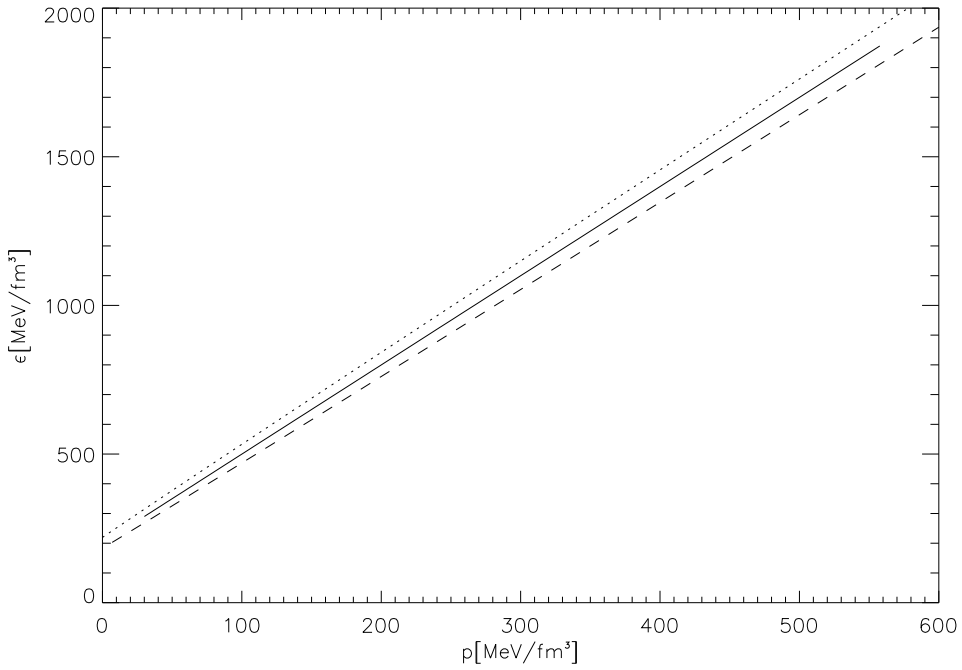

Figure 3.3: Pressure versus energy density relation for the MIT bag model (lines same as in figure 3.2)

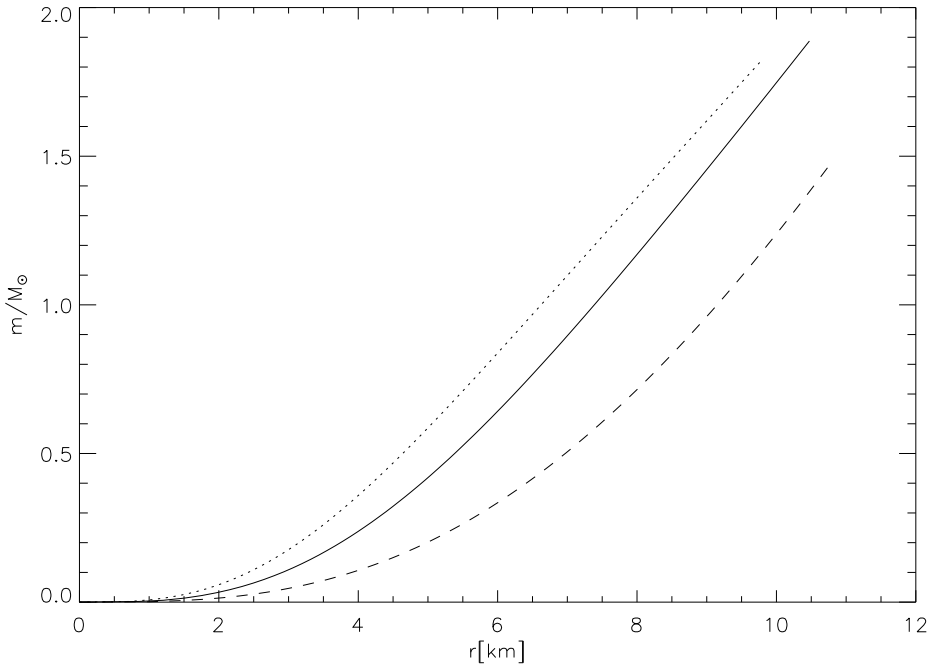

Figure 3.4: Enclosed mass versus distance from the center relationship for the MIT bag model with $a_4 = 0.6$, $a_2 = (100\ \text{MeV})^2$, $B_{\text{eff}}^{1/4} = 145$ MeV. The different curves depict different values of h_c, and they end at the surface of the star. For the solid line $h_c = 0.452$, for the dotted line $h_c = 0.6$ and for the dashed line $h_c = 0.2$.

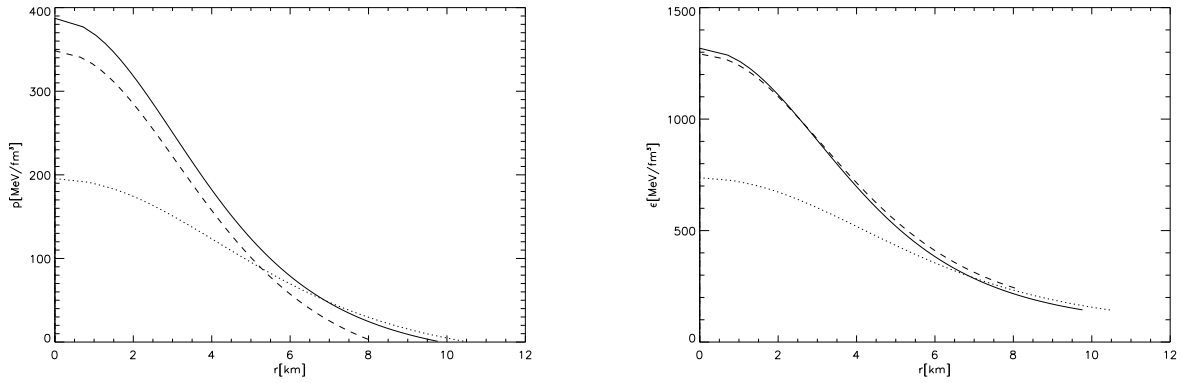

(a) $\mu - p$ relation **(b)** $\mu - \varepsilon$ relation

Figure 3.5: Pressure and energy density versus distance from the center relation for the MIT bag model. $a_4 = 0.6$ and $a_2 = (100\ \text{MeV})^2$ for all lines For the solid line $h_c = 0.6$ and the dotted line $h_c = 0.452$), $B_{\text{eff}}^{1/4} = 145$ MeV. For the dashed line $h_c = 0.471$ and $B_{\text{eff}}^{1/4} = 165$ MeV.

3.4 Strange or quark stars

It has been proposed by Witten that strange matter instead of ^{56}Fe might be the true ground state of matter [30] (the so-called "'strange matter hypothesis"'). There are generally two possibilities for this to occur in neutron stars [14]: Strange matter could be stable at very large pressures. In this case, we expect a first-order transition at some density. It is also possible that there is a mixed phase, or there might be multiple transitions between strange and hadronic matter if there is a region in which the equation of state for strange and hadronic matter are very similar, resulting in a star that has several layers of both kinds of matter [2]. The question is whether the density in the core of a neutron star is large enough to allow the transition. As lattice QCD is not well understood at neutron star densities, this question remains unanswered to date. The other possibility is that quark matter in bulk is already stable and bound by the strong interaction at zero pressure. Here, using the MIT bag model, it is possible to obtain a parameter window (the parameters being a_4, a_2 and B_{eff}) within which bulk strange matter is stable at zero pressure [9]. This would be possible if it had an energy per baryon that is less than 930 MeV. On the other hand, nonstrange matter needs to have an energy per baryon higher than 934 MeV, otherwise atomic nuclei would not be stable [9]. These two requirements put constraints on the allowed values for the bag constant and a_2. These constraints have been analyzed by Farhi and Jaffe [9] and their calculations shall be explained here.

Given an equation of state $p(\mu)$ (as in the bag model), the number density is given by

$$n = \frac{\partial p}{\partial \mu}. \tag{3.32}$$

Using this the energy per baryon can be calculated as follows:

$$\frac{E}{1/3 \cdot n} = \frac{-p + \mu n}{n}. \tag{3.33}$$

Equilibrium requires $p = 0$, so

$$E/n \equiv \varepsilon = 3\mu, \tag{3.34}$$

which then allows to calculate the bag constant for a given energy density and given a_4 and a_2 by substituting $\mu = \varepsilon/3$ in equation 3.9:

$$B_{\text{eff,c}} = \frac{3}{4\pi^2} a_4 \left(\frac{\varepsilon}{3}\right)^4 - \frac{3}{4\pi^2} a_2 \left(\frac{\varepsilon}{3}\right)^2. \tag{3.35}$$

This means that the bag constant is a quartic function of the energy density and linear in both a_2 and a_4.

For nonstrange (2-flavor) quark matter, the equation of state is

$$p = \frac{1}{2\pi^2} a_4 \mu^4 - B_{\text{eff}}. \tag{3.36}$$

$\varepsilon = 3\mu$ is still valid here, so

$$B_{\text{eff,c}} = \frac{1}{2\pi^2} a_4 \left(\frac{\varepsilon}{3}\right)^4. \tag{3.37}$$

For $\varepsilon = 934$ MeV, this means $B_{\text{eff}} \approx (148 \text{ MeV})^4 \cdot \text{a}_4$, and as explained above, this sets a lower limit for the bag constant. For $a_4 = 0.63$, we obtain $B_{\text{eff}}^{1/4} \approx 132$ MeV.

The constraints set by the equations 3.35 and 3.37 are shown in figure 3.6.

In their paper, Farhi and Jaffe use a slightly more complicated model. They assume a Fermi gas model of $u-$, $d-$, $s-$quarks and electrons in chemical equilibrium. As explained above, under the conditions of chemical equilibrium und charge neutrality, there is only one independent chemical potential, for example the strange quark chemical potential, which can be calculated using QCD perturbation theory. However, these modifications do not change the results appreciably, since the electron chemical potential turns out to be very small compared to the others. This is because quark matter in bulk contains almost equal numbers of up, down and strange quarks. Near the surface of a star, however, this is not the case anymore, and electrons are required for charge neutrality. It is therefore necessary to take surface effects into account [9].

A viable alternative for the surface of the star is a mixed phase that is not locally neutral, but still fulfills global charge neutrality. Such a phase would consist of quark nuggets inside an electron sea and the crust would be about 100 m thick [14].

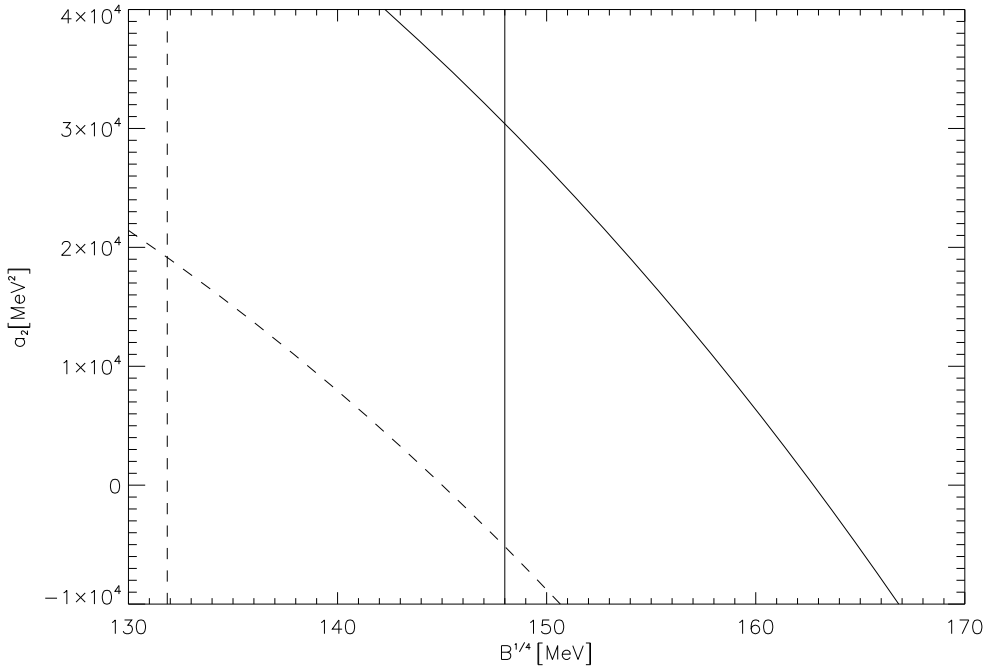

Figure 3.6: Constraints on the bag constant and a_2 for $a_4 = 1.0$ (solid line) and $a_4 = 0.63$ (dashed line). The vertical lines are the two flavor constraint and sets a lower limit for the bag constant, the curves are the three flavor constraint. The region between a vertical line and a curve is the allowed region for stable strange matter for each value of a_4. Note that hybrid stars could still exist right of the curves.

3.5 The maximally compact equation of state

The classic MIT bag model can be generalized by using the following equation of state [19]:

$$p = \begin{cases} 0 & if \quad \varepsilon \leq \varepsilon_0 \\ s(\varepsilon - \varepsilon_0) & if \quad \varepsilon > \varepsilon_0. \end{cases} \tag{3.38}$$

Here, s is the square of the speed of sound since

$$s = \frac{\partial p}{\partial \varepsilon} = c_s^2 \tag{3.39}$$

and ε_0 is a paramter. In case of the simple bag model presented above, we have $s = 1/3$ and $\varepsilon_0 = 4B_{\text{eff}}$. Apart from the bag model, this generalization also encompasses the so-called maximally compact equation of state ($s = 1$). It is of interest because causality requires $s \leq 1$ (i.e. the speed of sound is smaller than the speed of light). Therefore, it is maximally stiff where $\varepsilon > \varepsilon_0$ and maximally soft below that limit [22]. This leads to maximally compact

stars, i.e. the stars with the maximum mean density [19]. Integrating equation 2.11 in this case yields

$$p = t^{-1}\varepsilon_0(e^{ht} - 1), \tag{3.40}$$

$$\varepsilon = t^{-1}\varepsilon_0(s^{-1}e^{ht} + 1), \tag{3.41}$$

where $t = 1 + 1/s$. Results for the maximally compact equation of state (and for other choices s) can be found in [19]. An important result is that the central energy density $\varepsilon_{\max}$ of the maximum mass star must be inversely proportional to the square of the maximum mass, $\varepsilon_{\max} M_{\max}^2 = const.$ The constant depends on the choice of s and decreases with decreasing s. Note that the maximum mass star also has the maximum central energy density. Since the maximally compact equation of state is assumed to be a reasonable approximation for the possible maximum mass under the assumption of causality, the highest measured maximum mass (currently $(1.97 \pm 0.04)M_\odot$ [8]) also gives an estimate for the maximum central energy density in any star [19]. The relationship between the maximum mass and the maximum central density will be further examined in the following chapters.

3.6 Other models of the nucleon

An obvious extension of the bag model discussed above is to make the bag constant density dependent [26], for example as suggested in [4]:

$$B(\rho) = B_{\text{as}} + (B_0 - B_{\text{as}}) \exp(-\beta x^2), \tag{3.42}$$

where $x = \rho/\rho_0$ is the normalized baryon number density (ρ_0 being the baryon number density for nuclear matter), $B_{\text{as}} = 38$ MeV/fm^3, $B_0 = 200$ MeV/fm^3, $\beta = 0.14$. Other parametrizations are certainly possible (see for example [1], [21]). This generally leads to a stiffer equation of state and thus to lager masses and radii [26], but the difference is not significant [2].

Another option are NJL-type models that are mainly useful to describe chiral symmetry breaking in QCD. However, unlike the MIT bag model, they generally do not model confinement, making them applicable only in situations where confinement is not as relevant as chiral symmetry breaking [3]. Studies using the NJL model find maximum masses around $1.6M_\odot$ [13].

4 Dependence of the maximum mass on the parameters

In this chapter, the dependence of the maximum mass on the three parameters a_4, a_2 and B_{eff} in the MIT bag model shall be examined [2], [24], [29].

4.1 Estimates for the parameters

Perturbative calculations for a_4 find $a_4 \approx 0.63$ [2]. However, it is not clear whether perturbation theory is accurate at the densities that are expected to occur in neutron stars.

The quadratic coefficient a_2 includes the strange quark mass m_s and the pairing gap Δ. As this can be motivated by an expansion of the electron chemical potential in m_s/μ (see section 3.2), which requires $m_s < \mu$, we assume that the strange quark mass should be smaller than 300 MeV. Calculations with effective interactions predict $\Delta = 10 - 100$ MeV [2]. As a result, we expect a_2 to be between $-4 \cdot (100 \text{ MeV})^2$ and $(300 \text{ MeV})^2$. An upper limit for a_2 for stable strange stars is also given by the constraints analyzed in section 3.4. It is $3 \cdot 10^4$ MeV^2 for $a_4 = 1.0$ and smaller for smaller a_4.

In the classic MIT bag model, the bag constant is estimated to be about $(145 \text{ MeV})^4$ [7]. If the effective bag constant is taken to be dependent on the transition density from nuclear matter to quark matter, similar values are obtained [2].

4.2 Maximum mass contours

Following Weissenborn et al. [29], we want to obtain an allowed parameter window for a_4, a_2 and B_{eff}. This should take into account the conditions on the stability of quark stars from section 3.4 and permit a $1.97 M_\odot$ star. To do this, we keep one parameter fixed at all times, while going over a range of parameters for the others. Having calculated a matrix of maximum masses for the two non-fixed values, we use IDL's CONTOUR procedure to obtain contours of fixed maximum mass.

4.2.1 a_2 fixed

The results for fixed a_2 are shown in figure 4.1. The region between the two and the three flavor line allow stable strange matter. For $a_2 = (100 \text{ MeV})^2$, these requirements severely

restrict the allowed region of parameters. The $1.97M_\odot$ star requires the effective bag constant to be smaller than $(143\text{ MeV})^4$ and $a_4 \lesssim 0.87$. If the black widow pulsar's mass is confirmed to be $2.4M_\odot$ [28], strange stars would have to be ruled out under these assumptions. For $a_2 = -(100\text{ MeV})^4$, a $1.97M_\odot$ star would be permitted as long as $B_{\text{eff}} \lesssim (150\text{ MeV})^2$ and $a_4 \gtrsim 0.61$. A $2.4M_\odot$ star, however, would place more severe restrictions on the parameters, requiring $a_4 \lesssim 0.73$ and $B_{\text{eff}} \lesssim (137\text{ MeV})^4$ where $a_4 < 0.6$. Note that the slope of the contours changes when a_2 becomes negative: This makes sense if we assume that the slope is a monotonous function of a_2 since it must be zero for $a_2 = 0$ (in this case, the maximum mass does not depend on a_4). In conclusion, a larger value of a_4 results in a larger maximum mass if $a_2 > 0$ and it is the other way round for $a_2 < 0$. A larger effective bag constant generally results in a smaller maximum mass.

4.2.2 a_4 fixed

Next, we keep a_4 fixed (see figure 4.2). Generally, if a_2 increases, the maximum mass will decrease. As indicated by the small slope in the a_4 versus B_{eff} plot, the contours for $a_4 = 1.0$ and $a_4 = 0.63$ differ only minimally. However, the constraints are distinctly different. In the case of $a_4 = 1.0$, a $1.97M_\odot$ star requires $a_2 \lesssim 0.4 \cdot 10^{-4}$ and $B_{\text{eff}} \gtrsim (148\text{ MeV})^2$. For $a_2 = -3 \cdot 10^4\text{ MeV}^2$ we need $B_{\text{eff}} \lesssim (166\text{ MeV})^4$ and this value decreases as a_2 increases. Consequently, there is only a very small range of parameters that would be allowed here. $a_4 = 1.0$ would be ruled out by a $2.4M_\odot$ star, as we already saw above. $a_4 = 0.63$, however, permits a broader range of parameters: The three flavor constraint sets the maximum for $B_{\text{eff}}^{1/4}$ to be $139 - 160$ MeV, depending on a_2. The minimum is $B_{\text{eff}}^{1/4} \approx 132$ MeV. (Note the limiting values for B_{eff} were already calculated in section 3.4.) A $1.97M_\odot$ star now requires $B_{\text{eff}} \lesssim (156\text{ MeV})^4$. For a $2.4M_\odot$ star, $a_2 \lesssim 0.4 \cdot 10^4\text{ MeV}^2$ and $B_{\text{eff}} \lesssim (143\text{ MeV})^4$.

4.2.3 B_{eff} fixed

Last, we want to keep the effective bag constant fixed. This again leads to straight lines, and their slopes change sign at $a_2 = 0$ (see figure 4.3) for the same reason as before. Generally, it is again evident that a_4 only has a minor influence on the maximum mass, at least for the values of a_2 that were considered here. Of course, if a_2 turns out to be much larger, this statement would have to be reconsidered. As for the general behavior: An increase in a_4 accounts for a smaller maximum mass if $a_2 > 0$ and a higher maximum mass if $a_2 < 0$. A different bag constant does not change the general appearance of the curves, but again a higher bag constant results in a higher maximum mass. For $B_{\text{eff}} = (125\text{ MeV})^4$, a $1.97M_\odot$ star requires $a_2 \lesssim 3.6 - 5.7 \cdot 10^4\text{ MeV}^2$ (depending on a_4, $0.6 < a_4 < 1.0$) and a $2.4M_\odot$ star requires $a_2 \lesssim 1.4 - 1.8 \cdot 10^4\text{ MeV}^2$. For $B_{\text{eff}} = (165\text{ MeV})^4$, we need $a_2 \lesssim -6 \cdot 10^4\text{ MeV}^2$ for $1.97M_\odot$, so this can be ruled out considering the expected range of parameters for a_2.

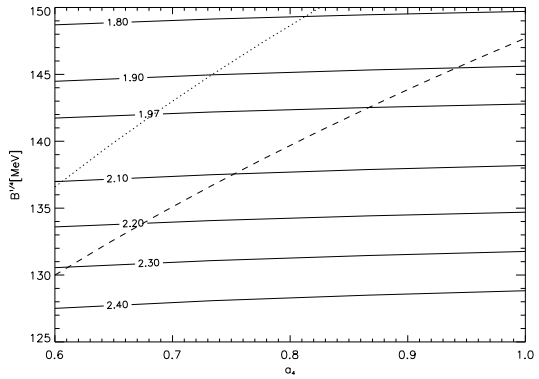

(a) $a_2 = (100MeV)^2$

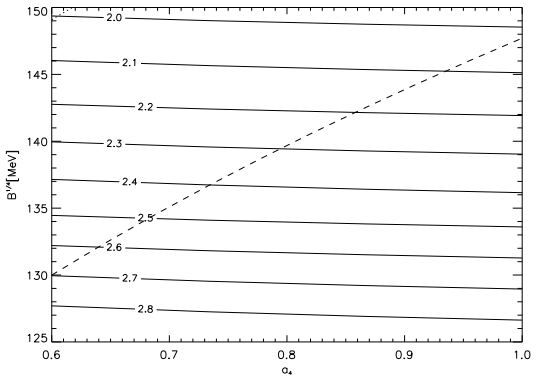

(b) $a_2 = -(100MeV)^2$

Figure 4.1: Maximum masses in units of solar masses in the MIT bag model as a function of the effective bag constant B_{eff} and the QCD correction a_4 for two different values of a_2. The dotted and dashed lines are the three and two flavor constraints as described in the text.

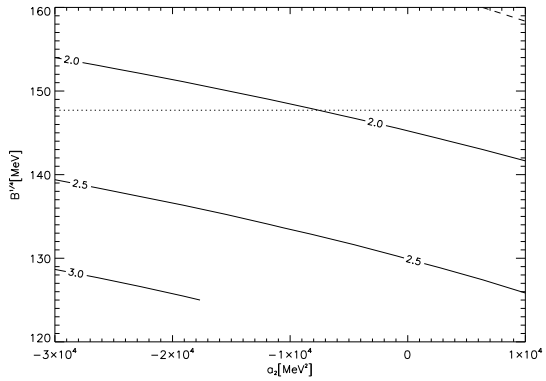

(a) $a_4 = 1.0$

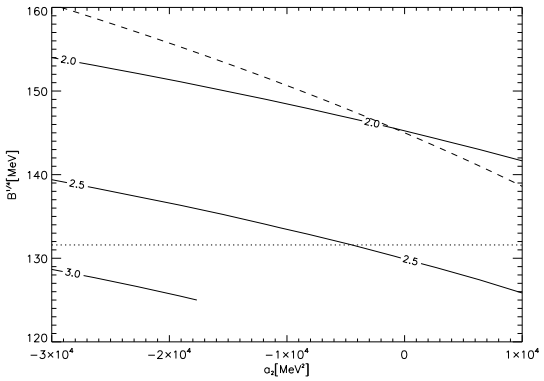

(b) $a_4 = 0.63$

Figure 4.2: Same as figure 4.1, but with fixed a_4. Here, the dashed line is the three flavor constraint, the other line is the two flavor constraint.

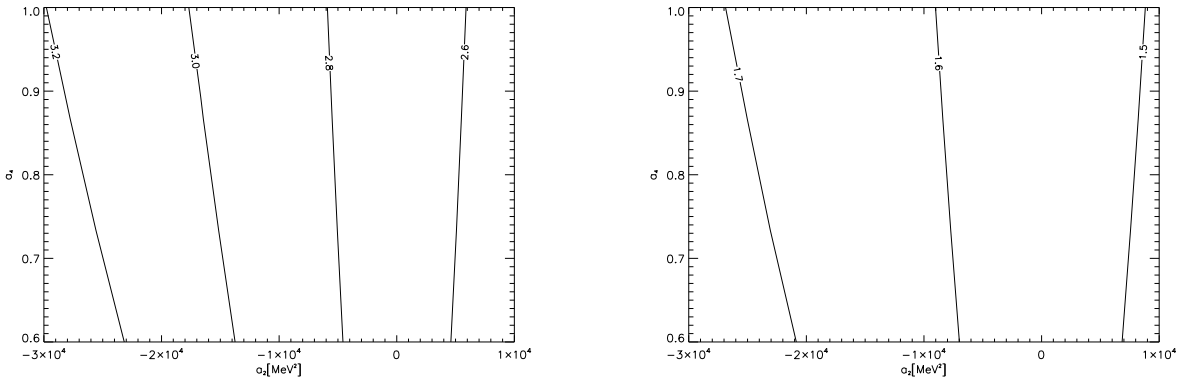

(a) $B_{\text{eff}}^{1/4} = 125$ MeV **(b)** $B_{\text{eff}}^{1/4} = 165$ MeV

Figure 4.3: Same as figure 4.1, but with fixed B_{eff}.

4.3 Scaling of the maximum mass with the parameters

For the before-mentioned general equation of state 3.38, we obtain [19]

$$M_{\max} \propto \frac{1}{\sqrt{\varepsilon_0}}, \tag{4.1}$$

$$R_{\max} \propto \frac{1}{\sqrt{\varepsilon_0}}, \tag{4.2}$$

with $R_{\max}$ denoting the radius of the maximum mass star, which is in general not the largest possible radius. These scaling relations can be deduced as follows [19]: We introduce dimensionless variables

$$x = r^2 \varepsilon_0, \tag{4.3}$$

$$y = m\sqrt{\varepsilon_0} \tag{4.4}$$

and write the TOV equations as

$$\frac{\partial x}{\partial h} = -\frac{2x(x^{1/2} - 2y)}{y + 4\pi x^{3/2} p/\varepsilon_0}, \tag{4.5}$$

$$\frac{\partial y}{\partial h} = 2\pi x^{1/2} \frac{\varepsilon}{\varepsilon_0}. \tag{4.6}$$

It is evident from equation 3.41 that for this equation of state $p(h)/\varepsilon_0$ and $\varepsilon(h)/\varepsilon_0$ are independent of ε_0. Therefore, the results for $x_{\max}$, $y_{\max}$ and $h_{\max}$ do not depend on ε_0. This explains the scaling relations presented above. The proportionality factors depend on the choice of s. If s increases, the maximum mass increases as well.

It follows directly that the so-called compactness $R_{\max}/M_{\max}$ is a constant for any s, independent of ε_0. It can be argued that the maximally compact equation of state predicts the minimum compactness of any neutron star [16], [19]. The minimum compactness is then 2.824. The question of the minimum compactness was already discussed in section 2.3.1. The reasoning presented here explains why $\beta = M/R$ should be smaller than 1/3 for realistic equations of state (see section 2.3.1). Requirements set by General Relativity were $R/M > 2$ (Schwarzschild condition) and $R/M > 9/4 = 2.25$ (finite central pressure).

Unfortunately, this technique cannot be applied for the MIT bag model equation of state. Nevertheless, it is possible to obtain some information by keeping two of the parameters fixed at a time.

4.3.1 Scaling with B_{eff}

First, we want to determine how the maximum mass scales with the effective bag constant B_{eff}. For $a_2 = (0\ \text{MeV})^2$, we know that

$$M_{\max} \propto B_{\text{eff}}^{-1/2}, \quad R_{\max} \propto B_{\text{eff}}^{-1/2}. \tag{4.7}$$

However, for different values of a_4 and a_2, this can no longer be assumed to be true (see figure 4.4). We choose

$$M_{\max} = \frac{a}{B_{\text{eff}}^b} \tag{4.8}$$

as an ansatz for the analytic description of the curves and use Mathematica's FindFit procedure to determine a and b for different values of a_2 and a_4. For $a_2 = (0\ \text{MeV})^2$ we find

$$M_{\max} = 1.24 \left(\frac{\varepsilon_s}{B_{\text{eff}}}\right)^{1/2} M_\odot, \tag{4.9}$$

where $\varepsilon_s = 150\ \text{MeV/fm}^3$. This is in agreement with the result found in [19]. For instance, for $a_4 = 0.6$ and $a_2 = (100\ \text{MeV})^2$ we find

$$M_{\max} = 0.6 \left(\frac{\varepsilon_s}{B_{\text{eff}}}\right)^{0.47} M_\odot \tag{4.10}$$

and $a_4 = 1.0$ and $a_2 = -(100\ \text{MeV})^2$ yields

$$M_{\max} = 2.07 \left(\frac{\varepsilon_s}{B_{\text{eff}}}\right)^{0.52} M_\odot. \tag{4.11}$$

The dependence of both a and b on a_2 appears to be linear in $B_{\text{eff}}^{1/4}$. A possible next step would be to obtain a fit for these parameters for different values of a_2. Then, another fit could be applied to the parameters of this fit to determine how they depend on a_4. However, this soon becomes very complicated: A linear fit to a and b depending on a_2 means that

$$M_{\max} = \frac{c_1 B_{\text{eff}}^{1/4} + c_2}{B_{\text{eff}}^{c_3 B_{\text{eff}}^{1/4} + c_4}}, \tag{4.12}$$

where each c_i will in turn depend on a_4. Thus, this method does not seem to promise to lead to real insight.

On a different note, plotting $R_{\max}$ versus $M_{\max}$ for different values of the parameters shows

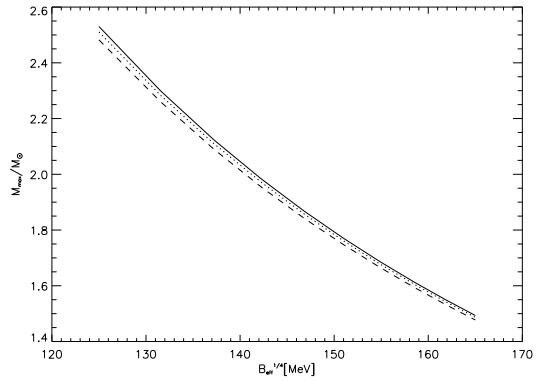

(a) $a_4 = 1.0$ (solid line), $a_4 = 0.8$ (dotted line), $a_4 = 0.6$ (dashed line), $a_2 = (100\ \text{MeV})^2$ for all lines

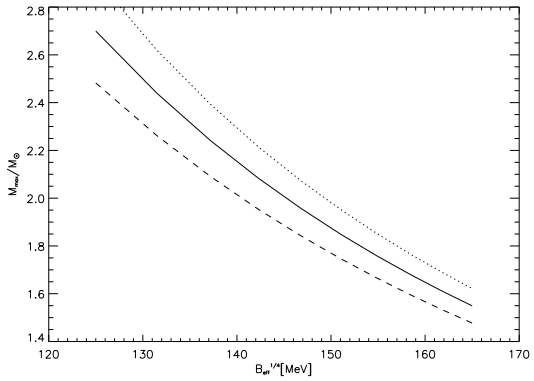

(b) $a_2 = (0\ \text{MeV})^2$ (solid line), $a_2 = (100\ \text{MeV})^2$ (dashed line), $a_2 = -(100\ \text{MeV})^2$ (dotted line), $a_4 = 0.6$ for all lines

Figure 4.4: Maximum mass versus effective bag constant relationship for different values of a_4 and a_2

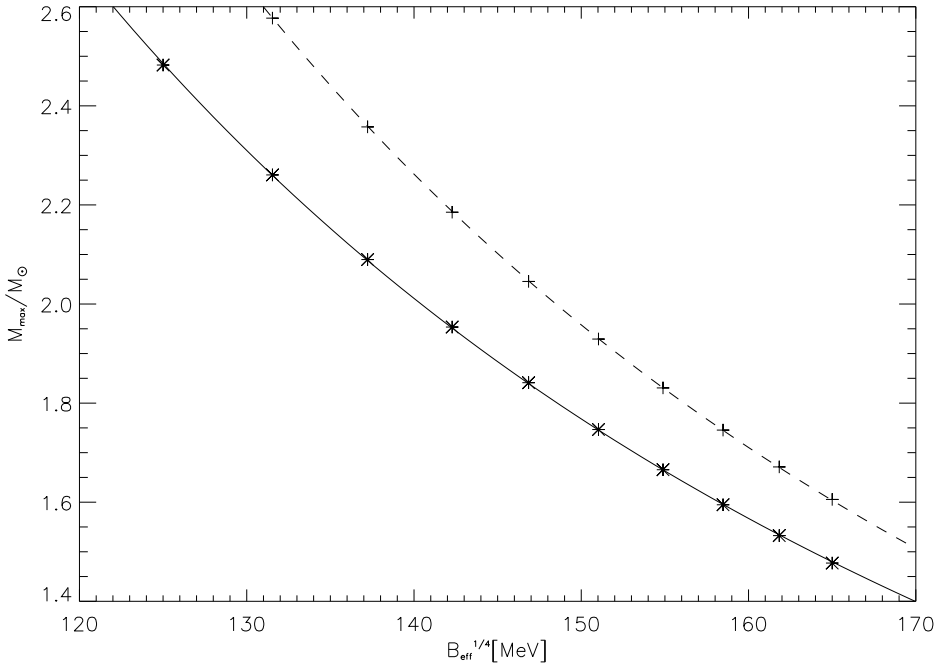

Figure 4.5: Fit for the maximum mass versus bag constant relationships for $a_4 = 1.0$ and $a_2 = -(100\ \text{MeV})^2$ (dashed line) and $a_4 = 0.6$ and $a_2 = (100\ \text{MeV})^2$ (solid line). The data points are the result of the numerical calculation.

that $R_{\max} \propto M_{\max}$ (see figure 4.6). Using

$$\frac{\partial M_{\max}}{\partial B_{\text{eff}}} = \frac{dM_{\max}}{dR_{\max}} \frac{\partial R_{\max}}{\partial B_{\text{eff}}} \tag{4.13}$$

we conclude that $R_{\max}$ scales with B_{eff} in the same way as $M_{\max}$ does.

4.3.2 Scaling with a_2

Next, we want to analyze the dependence of $M_{\max}$ on a_2. Here, the relation between $M_{\max}$ and a_2 appears to be linear in $B_{\text{eff}}^{1/4}$. Figure 4.7 shows this for different values of a_4 and B_{eff}. Note that the axis intercept is given by equation 4.9. The slope depends on both a_4 and B_{eff}, though, and it increases as B_{eff} or a_4 increase.

A fit for $a_4 = 1.0$ and $B_{\text{eff}}^{1/4} = 165$ MeV gives a slope of $-5.608\ M_\odot/\text{MeV}$ and an axis intercept of $1.55 M_\odot$ (see figure 4.8), which agrees with equation 4.9.

4.3.3 Scaling with a_4

In case of the dependence of the maximum mass on a_4, we expect different behavior for $a_2 > 0$ and $a_2 < 0$, as explained above. Figure 4.9 shows the $M_{\max}$ versus a_4 curve for different values of a_2 and B_{eff}. As observed before, the other parameters have a much greater influence on the maximum mass than does a_4. For the parameter range considered here, the difference between the maximum mass for $a_4 = 0.6$ and $a_4 = 1.0$ is at most about 1%. Of course, the difference is greater for larger a_2. However, even for $a_2 = \pm(300\ \text{MeV})^2$ the difference does not exceed 15% for realistic values of the bag constant.

For an analytic fit,

$$M_{\max} = c_1 a_4^2 + c_2 a_4 + c_3 \tag{4.14}$$

seems to be a reasonable ansatz, where c_1, c_2 and c_3 are constants that depend on a_2 and B_{eff}. Typical curves for both $a_2 > 0$ and $a_2 < 0$ are shown in figure 4.10, where the fitted constants are

$$c_1 = -0.038 M_\odot, \tag{4.15}$$
$$c_2 = 0.101 M_\odot, \tag{4.16}$$
$$c_3 = 1.430_\odot, \tag{4.17}$$

for $a_2 = (100\ \text{MeV})^2$ and

$$c_1 = 0.039 M_\odot, \tag{4.18}$$
$$c_2 = -0.102 M_\odot, \tag{4.19}$$
$$c_3 = 1.669 M_\odot, \tag{4.20}$$

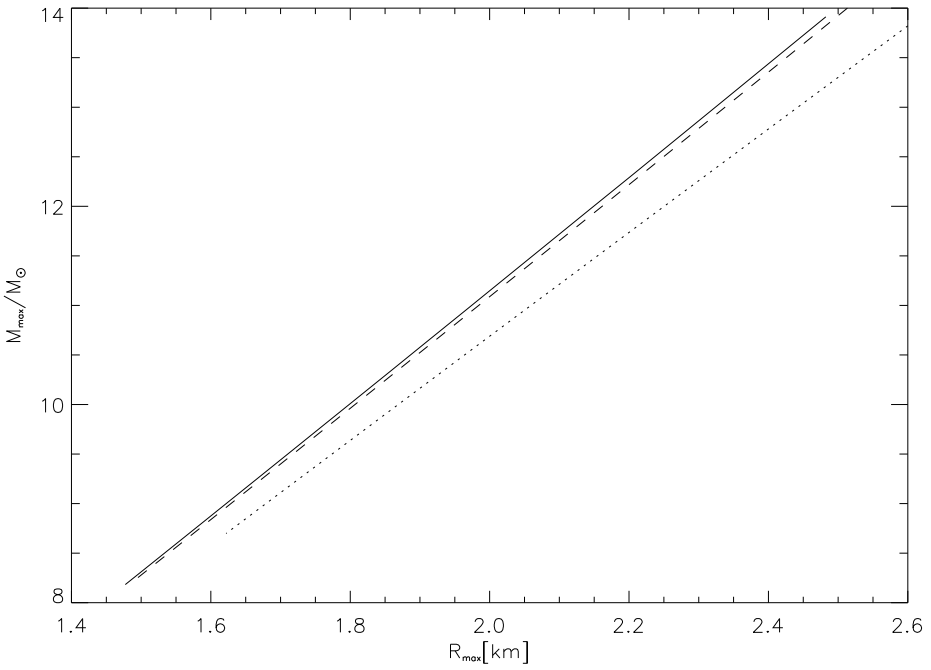

Figure 4.6: $R_{\max}$ versus $M_{\max}$ for $a_2 = (100\text{ MeV})^2$ and $a_4 = 0.6$ (solid line), $a_2 = (100\text{ MeV})^2$ and $a_4 = 1.0$ (dashed), $a_2 = -(100\text{ MeV})^2$ and $a_4 = 0.6$ (dotted). $B_{\text{eff}}^{1/4}$ ranges from 125 MeV to 165 MeV.

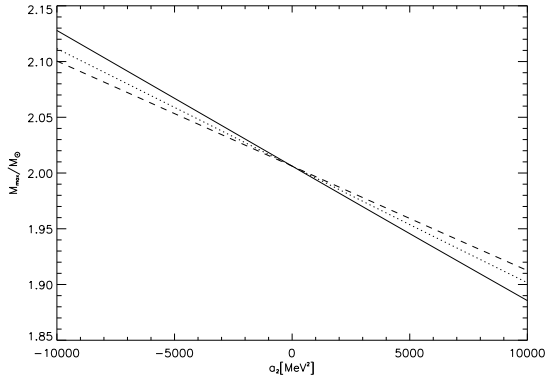

(a) $a_4 = 1.0$ (solid line), $a_4 = 0.8$ (dotted line), $a_4 = 0.6$ (dashed line), $a_2 = (100\text{ MeV})^2$ for all lines

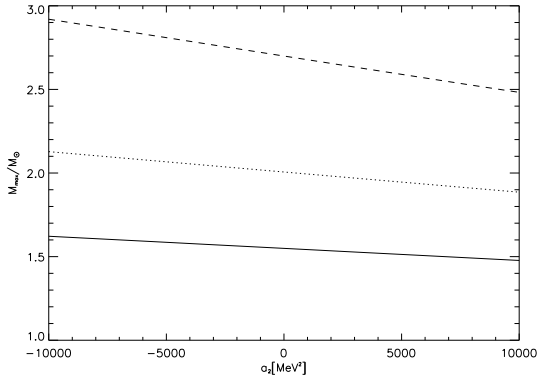

(b) $B_{\text{eff}} = (165\text{ MeV})^4$ (solid line), $B_{\text{eff}} = (145\text{ MeV})^4$ (dotted line), $B_{\text{eff}} = (125\text{ MeV})^4$ (dashed line), $a_4 = 0.6$ for all lines

Figure 4.7: Maximum mass versus a_2 relationship for different values of a_4 and B_{eff}

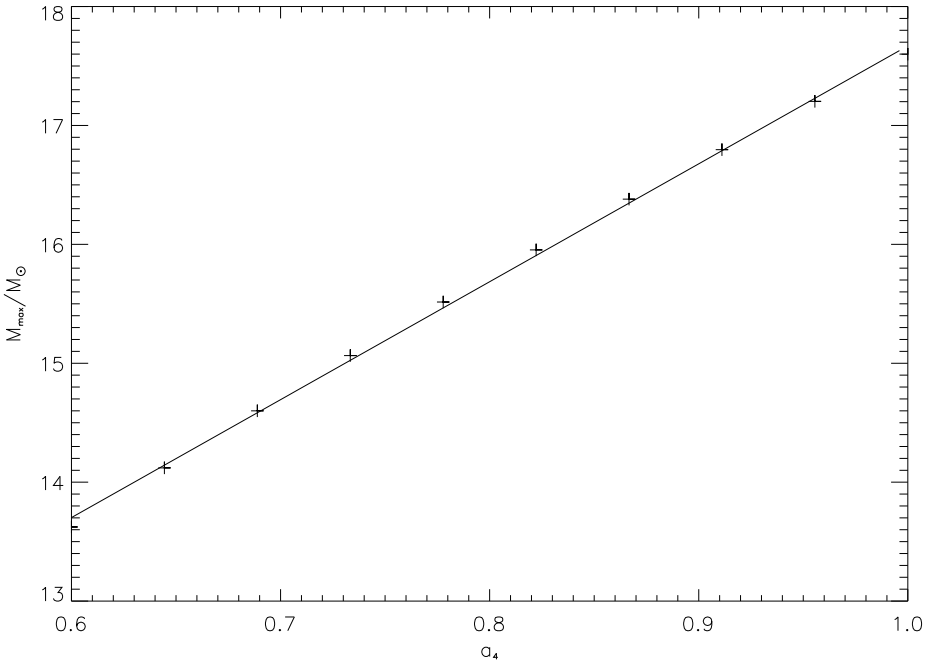

Figure 4.8: Dependence of the maximum mass on a_2 for $a_4 = 1.0$ and $B_{\rm eff}^{1/4} = 165$ MeV.

for $a_2 = -(100\ \text{MeV})^2$.

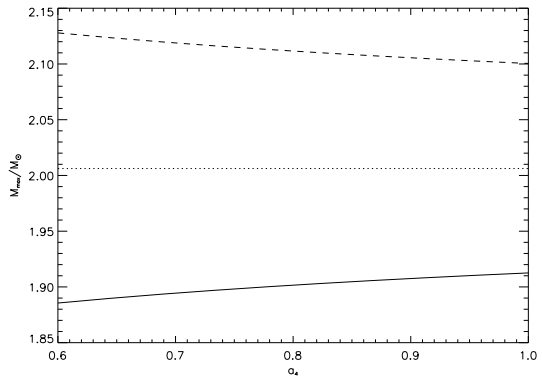

(a) $a_2 = (100\ \text{MeV})^2$ (solid line), $a_2 = (0\ \text{MeV})^2$ (dotted line), $a_4 = -(100\ \text{MeV})^2$ (dashed line), $B_{\text{eff}} = (145\ \text{MeV})^4$ for all lines

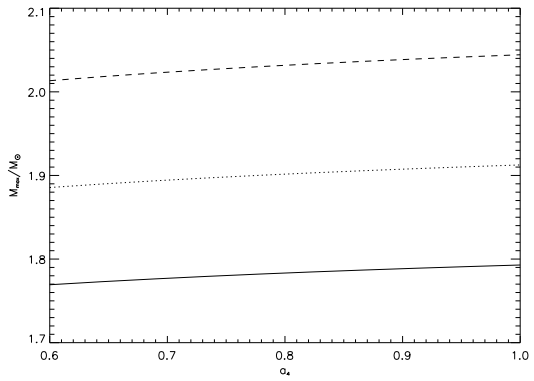

(b) $B_{\text{eff}} = (150\ \text{MeV})^4$ (solid line), $B_{\text{eff}} = (145\ \text{MeV})^4$ (dotted line), $B_{\text{eff}} = (140\ \text{MeV})^4$ (dashed line), $a_2 = (100\ \text{MeV})^2$ for all lines

Figure 4.9: Maximum mass versus a_4 relationship for different values of a_2 and B_{eff}

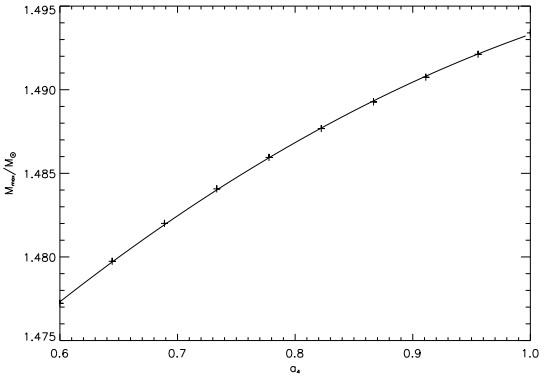

(a) $a_2 = (100\ \text{MeV})^2$

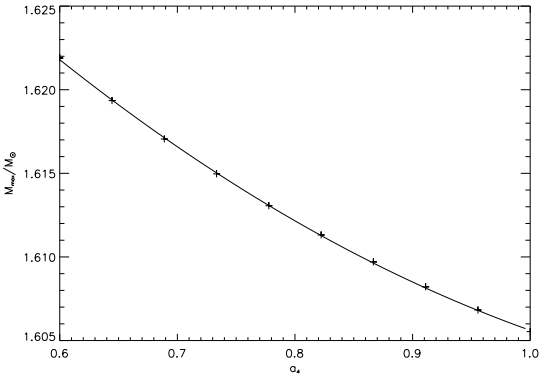

(b) $a_2 = -(100\ \text{MeV})^2$

Figure 4.10: Dependence of the maximum mass on a_4 for $B_{\text{eff}}^{1/4} = 165$ MeV.

4.4 Summary

The general dependence of the maximum mass on the parameters can be summarized as follows

$$a_4 \uparrow \Rightarrow \begin{cases} M_{\max} \uparrow & \text{if } a_2 > 0 \\ M_{\max} \downarrow & \text{if } a_2 < 0 \end{cases} \tag{4.21}$$

$$a_2 \downarrow \Rightarrow M_{\max} \downarrow \tag{4.22}$$

$$B_{\text{eff}} \uparrow \Rightarrow M_{\max} \downarrow . \tag{4.23}$$

A $1.97M_\odot$ star is generally possible in the context of the MIT bag model. However, it places severe restrictions on the parameters. For the effective bag constant, a value smaller than about $(150\ \mathrm{MeV})^4$ seems to be necessary, although configurations with a larger bag constant are possible. a_2 is also likely to be close to $(0\ \mathrm{MeV})^2$ or smaller, so a large pairing gap would be required. a_4 should be significantly smaller than 1.0. A $2.4M_\odot$ restricts the parameters even further, making pure quark stars seem unlikely. This would not rule out the possibility of quark matter in the cores of hybrid stars, though.

We saw that the influence of a_4 on the maximum mass is relatively small compared to the other parameters for realistic values of a_2. However, this is only true for pure quark stars. In hybrid stars, a_4 has a major influence on the density at which the transition from nuclear to quark matter occurs. This in turn results in significantly higher maximum masses for smaller a_4 [2].

5 Thermodynamic quantities of quark stars

There are several thermodynamic quantities that are of interest in the physics of neutron stars: pressure, energy and number density and the chemical potential. All of these quantities reach their maximum at the center of the maximum mass neutron star. To determine these maximum values for a specific equation of state, we must therefore first calculate the maximum mass. Using Newton's method, we can then determine the corresponding maximum value of h, which immediately gives us the maximum pressure and energy density. The maximum chemical potential is given by $\mu_{\max} = \mu_0 e^{h_{\max}}$. The maximum number density is given by [19]

$$n_{\max} = \frac{\varepsilon_{\max} + p_{\max}}{\mu_{\max}}. \tag{5.1}$$

5.1 A lower limit for the central energy density

A question of special interest is how large the central energy density in a star can be. Upper and lower limits to this quantity could eliminate possible equations of state that predict lower or higher values for the central energy density. An upper limit might furthermore set an upper limit to the density of cold baryonic matter [20]. Obviously, the central energy density must be larger than the average density

$$\bar{\varepsilon} = \frac{3M}{4\pi R^3}. \tag{5.2}$$

The largest observed redshift from a neutron star sets a lower limit to M/R. With $z = 0.35$ [6], this results in [20]

$$\varepsilon_c > 0.953 \ \frac{\text{GeV}}{\text{fm}^3} \left(\frac{M_\odot}{M}\right)^2. \tag{5.3}$$

This means that a typical $1.5 M_\odot$ would need to have a central density that is larger than 0.423 GeV/fm^3, with the lower limit for the central density decreasing for larger stars.

5.2 Scaling relations for the general equation of state 3.38

For the before-mentioned general equation of state 3.38, we obtain directly from equations 3.41 and 5.1:

$$\varepsilon_{\max} \propto \varepsilon_0, \tag{5.4}$$

$$p_{\max} \propto \varepsilon_0, \tag{5.5}$$

$$\mu_{\max} \propto \mu_0, \tag{5.6}$$

$$n_{\max} \propto \frac{\varepsilon_0}{\mu_0}. \tag{5.7}$$

The quantity $\varepsilon_{\max} M_{\max}^2$ is of special interest here. From the relations given above, we conclude that it is a constant for given s, i.e. it does not depend on ε_0. Specifically,

$$M_{\max} = \sqrt{\frac{c_1(s)}{\varepsilon_{\max}}} M_\odot, \tag{5.8}$$

where $c_1(s)$ is a constant that depends on s,

$$c_1(1) = 3.034 \cdot (4.09)^2 \cdot 150 \ \frac{\text{MeV}}{\text{fm}^3} = 7.612 \ \frac{\text{GeV}}{\text{fm}^3}, \tag{5.9}$$

$$c_1(1/3) = 4.826 \cdot (2.48)^2 \cdot 150 \ \frac{\text{MeV}}{\text{fm}^3} = 4.452 \ \frac{\text{GeV}}{\text{fm}^3}. \tag{5.10}$$

Note that the $s = 1$ case is very similar to the expression for the Tolman VII solution (equation 2.28).

If we assume that the maximally compact equation of state gives an upper limit for the maximum mass, then it would be logical if the corresponding $\varepsilon_{\max}$ described the largest possible energy density in any neutron star. Under this assumption, we find

$$\varepsilon_{\max} < \left(\frac{4.09 M_\odot}{M_{\max}}\right)^2 \cdot 150 \ \frac{\text{MeV}}{\text{fm}^3} \tag{5.11}$$

as a limit for central energy density. Obviously, this limit will decrease as larger stars are measured. For example, the newly measured $1.97 M_\odot$ star implies that

$$\varepsilon_{\max} < 1.97 \ \frac{\text{GeV}}{\text{fm}^3}. \tag{5.12}$$

For a $2.4 M_\odot$ star, this limit would even have to decrease to

$$\varepsilon_{\max} < 1.33 \ \frac{\text{GeV}}{\text{fm}^3}. \tag{5.13}$$

5.3 An upper limit for the central energy density and pressure

Now, the next question is if there is a similar relation for the bag model from equation 3.9 (i.e. including the a_2 term). It is clear that a_4 alone will not change the structure of the star because it does not influence the equation of state. Therefore, we calculate the central energy density and the maximum mass for different values of the parameters. The results can be seen in figure 5.1. For each set of data points, a_2 was kept fixed while iterating over $B_{\text{eff}}^{1/4}$ from 100 MeV to 200 MeV. a_4 was also kept fixed. The calculation was repeated for different values of a_4, but this does have a significant influence on the results.

We find that even when taking a_4 and a_2 into account, the equation obtained for the classic bag model remains valid, i.e.

$$M_{\text{max}}^2 \varepsilon_{\text{max}} = 4.452 \ \frac{\text{GeV}}{\text{fm}^3} M_\odot. \tag{5.14}$$

Therefore, for $M_{\text{max}} > 1.97 M_\odot$, the central density of a quark star should satisfy

$$\varepsilon_{\text{max}} < 1.147 \ \frac{\text{GeV}}{\text{fm}^3} \tag{5.15}$$

for any set of parameters in the bag model, and for $M_{\text{max}} > 2.4 M_\odot$

$$\varepsilon_{\text{max}} < 0.773 \ \frac{\text{GeV}}{\text{fm}^3}. \tag{5.16}$$

The same analysis can be done for $p_{\text{max}} M_{\text{max}}^2$. According to equation 5.7, this is also a constant in the equation of state from equation 3.38. Thus,

$$M_{\text{max}} = \sqrt{\frac{c_2(s)}{\varepsilon_{\text{max}}}} M_\odot, \tag{5.17}$$

where

$$c_2(1) = 2.034 \cdot (4.09)^2 \cdot 150 \ \frac{\text{MeV}}{\text{fm}^3} = 5.094 \ \frac{\text{GeV}}{\text{fm}^3}, \tag{5.18}$$

$$c_2(1/3) = 1.275 \cdot (2.48)^2 \cdot 150 \ \frac{\text{MeV}}{\text{fm}^3} = 1.176 \ \frac{\text{GeV}}{\text{fm}^3}. \tag{5.19}$$

The values used to calculate c_2 are again taken from [19]. Figure 5.1 shows the results in this case. Here, the curve for $s = 1/3$ still provides a reasonable approximation for the generalized bag model, independent of the parameters, although the deviation is greater than for the central energy density.

Now that we know how ε_{max} and p_{max} depend on M_{max}, we can use the scaling relations found in section 5.7 to determine how ε_{max} and p_{max} depend on the parameters in the MIT

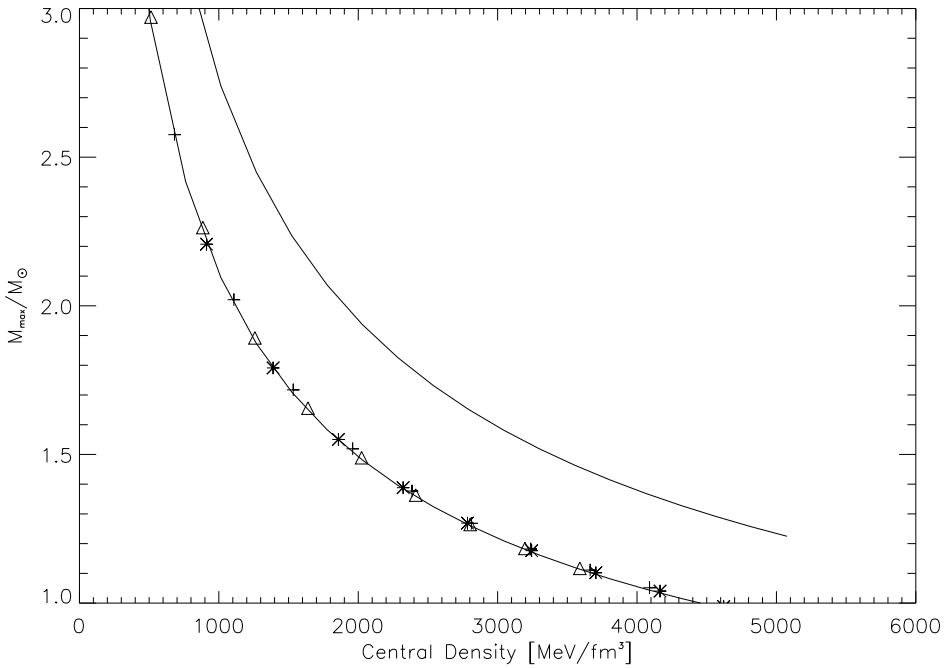

Figure 5.1: Central density versus maximum mass for $s = 1$ (upper curve), $s = 1/3$ (lower curve) and the bag model 3.9 (crosses: $a_2 = (0\ \text{MeV})^2$, stars: $a_2 = (150\ \text{MeV})^2$, triangles: $a_2 = (150\ \text{MeV})^2$, $a_4 = 1.0$).

bag model. For example, we found that $M_{\max} \propto B_{\text{eff}}^{-b}$, therefore

$$\varepsilon_{\max}, p_{\max} \propto B_{\text{eff}}^{2b}. \tag{5.20}$$

Also, the maximum central pressure must be proportional to the maximum central density.

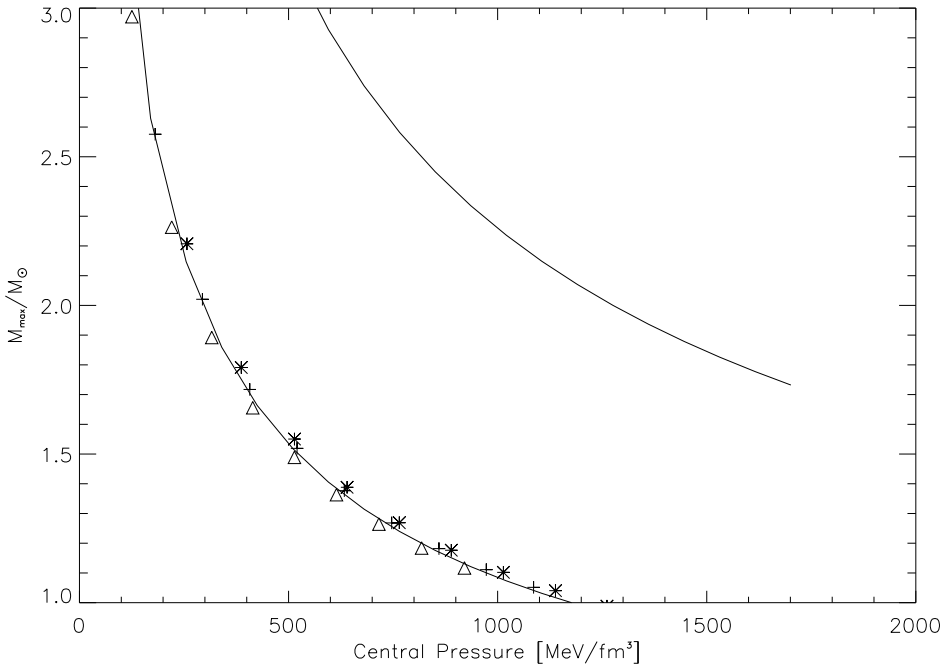

Figure 5.2: Central pressure versus maximum mass relation, lines and data points as in figure 5.1.

6 Summary and conclusions

We have studied strange stars under the assumption of the strange matter hypothesis. For the equation of state, we used an MIT bag model that takes QCD corrections, the strange quark mass and color superconductivity into account.

We find that the recent measurement of a $1.97M_\odot$ star cannot rule out the possibility of pure quark stars, but it does place requirements on the parameters of the bag model. For example, QCD corrections appear to be necessary, as well as a large pairing gap. We furthermore expect a bag constant that is smaller than $(150\text{ MeV})^4$. However, all of these requirements are well within the range of predictions for the parameters from both perturbative calculations and experiments. This is not longer true if a much larger neutron star were measured: Our calculations show that a $2.4M_\odot$ star would set very strict constraints on the parameters that make a pure quark star seem rather unlikely.

We also found parametrizations for the maximum mass curve depending on each one of the three parameters. An extension of the method applied here to find a parametrization of M_{max} depending on two or all of the parameters did not appear promising. A different ansatz, however, might lead to different results. A possible approach would be to first parametrize the (almost) linear energy density versus pressure relationship depending on the parameters, and then use $\varepsilon = c \cdot p + 3B_{\text{eff}}$ as equation of state, possibly leading to an easy scaling relation with c.

Our analysis of the central pressure and density versus radius relations showed that these relations are independent of the bag model's parameters. With a maximum mass of more than $1.97M_\odot$, it can be concluded that the central energy density in a quark star described by the MIT bag model cannot be larger than 1.147 GeV/fm^3. At this point, an analysis using other quark matter models such as the NJL model or a model with a density-dependent bag constant might be in order to determine whether this limit is model-independent.

Furthermore, the analysis could be extended to hybrid stars, i.e. the case where strange matter is stable at some finite pressure. These stars would consist of a quark core, possibly a mixed phase and a hadronic crust. The density at which the transition might occur is uncertain, but a two solar mass star is definitely possible in this context [2]. There are different possibilities for the equation of state for the nuclear phase: One could use the Akmal-Pandharipande-Ravenhal equation of state [2] or employ a simple quadratic approximation [19]. Modifications to the bag model (for example treating the bag constant as dependent on the transition density) might be in order. It would be interesting to see if the $s = 1/3$ central energy density–maximum mass constraint continues to hold in the case of hybrid stars, as this constraint is much more restrictive than the maximally compact constraint.

Of course, the observation of heavier neutron stars would set even tighter constraints on the thermodynamic quantities, so the precise measurement of neutron star masses promises to remain an exciting field for some years to come.

Bibliography

[1] R. Aguirre. Chiral symmetry and strangeness content in nuclear physics parametrized by a medium dependent bag constant. *Phys. Lett.*, B559:207–213, 2003. doi: 10.1016/S0370-2693(03)00345-9.

[2] Mark Alford, Matt Braby, Mark Paris, and Sanjay Reddy. Hybrid Stars that Masquerade as Neutron Stars. *The Astrophysical Journal*, 629(2):969, 2005. URL `http://stacks.iop.org/0004-637X/629/i=2/a=969`.

[3] Michael Buballa. NJL-model analysis of dense quark matter. *arXiv:hep-ph/0402234v2*, 2004.

[4] G. F. Burgio, M. Baldo, P. K. Sahu, A. B. Santra, and H. J. Schulze. Maximum mass of neutron stars with a quark core. *Phys. Lett.*, B526:19–26, 2002. doi: 10.1016/S0370-2693(01)01479-4.

[5] A. Chodos, R. L. Jaffe, K. Johnson, C. B. Thorn, and V. F. Weisskopf. New extended model of hadrons. *Phys. Rev. D*, 9(12):3471–3495, Jun 1974. doi: 10.1103/PhysRevD.9.3471.

[6] J. Cottam, F. Paerels, and M. Mendez. Gravitationally redshifted absorption lines in the X-ray burst spectra of a neutron star. *Nature*, 420:51–54, 2002. doi: 10.1038/nature01159.

[7] T. DeGrand, R. L. Jaffe, K. Johnson, and J. Kiskis. Masses and other parameters of the light hadrons. *Phys. Rev. D*, 12(7):2060–2076, Oct 1975. doi: 10.1103/PhysRevD.12.2060.

[8] P.B. Demorest, T. Pennucci, S.M. Ransom, M.S.E. Roberts, and J.W.T. Hessels. A two-solar-mass neutron star measured using Shapiro delay. *Nature*, 467:1081, 2010.

[9] Edward Farhi and R. L. Jaffe. Strange matter. *Phys. Rev. D*, 30(11):2379–2390, Dec 1984. doi: 10.1103/PhysRevD.30.2379.

[10] Norman K. Glendenning. Fast pulsars, strange stars: An Opportunity in radio astronomy. *Mod. Phys. Lett.*, A5:2197–2208, 1990. doi: 10.1142/S021773239000250X.

[11] Norman K. Glendenning. First-order phase transitions with more than one conserved charge: Consequences for neutron stars. *Phys. Rev. D*, 46(4):1274–1287, Aug 1992. doi: 10.1103/PhysRevD.46.1274.

[12] Øyvind Grøn and Sigbjorn Hervik. *Einstein's General Theory of Relativity: With Modern Applications in Cosmology*. Springer, 2007.

[13] M. Hanauske, L. M. Satarov, I. N. Mishustin, Horst Stoecker, and W. Greiner. Strange quark stars within the Nambu-Jona-Lasinio model. *Phys. Rev.*, D64:043005, 2001. doi: 10.1103/PhysRevD.64.043005.

[14] P. Jaikumar. Quark stars: features and findings. *The European Physical Journal C - Particles and Fields*, 49:199–203, 2007. ISSN 1434-6044. URL `http://dx.doi.org/10.1140/epjc/s10052-006-0064-y`. 10.1140/epjc/s10052-006-0064-y.

[15] K. Johnson. The M.I.T. Bag Model. *Acta Phys.Polon.*, 1975.

[16] Scott Koranda, Nikolaos Stergioulas, and John L. Friedman. Upper limits set by causality on the rotation and mass of uniformly rotating relativistic stars. *The Astrophysical Journal*, 488(2):799, 1997. URL `http://stacks.iop.org/0004-637X/488/i=2/a=799`.

[17] J. M. Lattimer and M. Prakash. Neutron Star Structure and the Equation of State. *The Astrophysical Journal*, 550(1):426, 2001. URL `http://stacks.iop.org/0004-637X/550/i=1/a=426`.

[18] J. M. Lattimer, M. Prakash, D. Masak, and A. Yahil. Rapidly rotating pulsars and the equation of state. *The Astrophysical Journal*, 355:241–254, May 1990. doi: 10.1086/168758.

[19] James M. Lattimer and M. Prakash. What a Two Solar Mass Neutron Star Really Means. *arXiv:1012.3208v1*, 2010.

[20] James M. Lattimer and Madappa Prakash. Ultimate Energy Density of Observable Cold Baryonic Matter. *Phys. Rev. Lett.*, 94(11):111101, Mar 2005. doi: 10.1103/PhysRevLett.94.111101.

[21] Yu-xin Liu, Dong-feng Gao, and Hua Guo. Density dependence of nucleon bag constant, radius and mass in an effective field theory model of QCD. *Nucl. Phys.*, A695:353–364, 2001. doi: 10.1016/S0375-9474(01)01120-4.

[22] P. S. Negi and M. C. Durgapal. Equation of state of dense nuclear matter and an upper bound on neutron star masses. *Astrophysics and Space Science*, 275:299–318, February 2001.

[23] J. R. Oppenheimer and G. M. Volkoff. On Massive Neutron Cores. *Phys. Rev.*, 55(4):374–381, Feb 1939. doi: 10.1103/PhysRev.55.374.

[24] Feryal Ozel, Dimitrios Psaltis, Scott Ransom, Paul Demorest, and Mark Alford. The Massive Pulsar PSR J1614-2230: Linking Quantum Chromodynamics, Gamma-ray Bursts, and Gravitational Wave Astronomy. *arXiv:1010.5790v1*, 2010.

[25] Sergey A. Postnikov. Topics in the Physics and Astrophysics of Neutron Stars. PhD thesis, Ohio University, 2010.

[26] Nirvikar Prasad and R. S. Bhalerao. Strange stars with a density-dependent bag parameter. *Phys. Rev. D*, 69(10):103001, May 2004. doi: 10.1103/PhysRevD.69.103001.

[27] Clifford E. Rhoades and Remo Ruffini. Maximum mass of a neutron star. *Phys. Rev. Lett.*, 32(6):324–327, Feb 1974. doi: 10.1103/PhysRevLett.32.324.

[28] M. H. van Kerkwijk, R. P. Breton, and S. R. Kulkarni. Evidence for a Massive Neutron Star from a Radial-velocity Study of the Companion to the Black-widow Pulsar PSR B1957+20. *ApJ*, 728:95–+, February 2011. doi: 10.1088/0004-637X/728/2/95.

[29] Simon Weissenborn, Irina Sagert, Giuseppe Pagliara, Matthias Hempel, and Jurgen Schaffner-Bielich. Quark Matter In Massive Neutron Stars. 2011.

[30] Edward Witten. Cosmic separation of phases. *Phys. Rev. D*, 30(2):272–285, Jul 1984. doi: 10.1103/PhysRevD.30.272.

[31] Cheuk-Yin Wong. *Introduction to High-Energy Heavy-Ion Collisions*. World Scientific Publishing Co. Pte. Ltd., 1994.